Wavelet Method for the Solution of Caputo and Caputo-Hadamard Fractional Differential Equations

By

Adab Hussain

(Registration No: 00000403065)

Department of Mathematics

School of Natural Sciences

National University of Sciences and Technology (NUST)

Islamabad, Pakistan

(2024)

Wavelet Method for the Solution of Caputo and Caputo-Hadamard Fractional Differential Equations

By

Adab Hussain

(Registration No: 00000403065)

A thesis submitted to the National University of Sciences and Technology, Islamabad,

in partial fulfillment of the requirements for the degree of

Master of science in

Mathematics

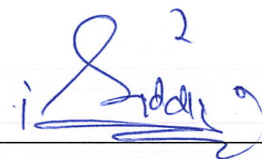Supervisor: Dr.Muhammad Israr

School of natural sciences

National University of Sciences and Technology (NUST)

Islamabad, Pakistan

(2024)

THESIS ACCEPTANCE CERTIFICATE

Certified that final copy of MS thesis written by **Adab Hussain** (Registration No **00000403065)**, of **School of Natural Sciences** has been vetted by undersigned, found complete in all respects as per NUST statutes/regulations, is free of plagiarism, errors, and mistakes and is accepted as partial fulfillment for award of MS/M.Phil degree. It is further certified that necessary amendments as pointed out by GEC members and external examiner of the scholar have also been incorporated in the said thesis.
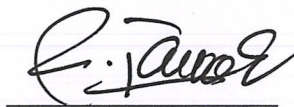
Signature: _____

Name of Supervisor: Dr. Muhammad Israr

Date: _____30-08-2024_____

Signature (HoD): _____

Date: 30/8/2024

Signature (Dean/Principal): _____

Date: _____02·09·2024_____

National University of Sciences & Technology

MS THESIS WORK

We hereby recommend that the dissertation prepared under our supervision by: Adab Hussain, Regn No. 00000403065 Titled Wavelet Methods for the Solution of Caputo and Caputo-Hadamard Fractional Differential Equations be Accepted in partial fulfillment of the requirements for the award of MS degree.

Examination Committee Members

1. Name: PROF. MUJEEB UR REHMAN   Signature:_____

2. Name: DR. MUHAMMAD ASIF FAROOQ   Signature:_____

Supervisor's Name DR. MUHAMMAD ISRAR   Signature:_____

_____
Head of Department

_____30/8/2024_____
Date

COUNTERSINGED

Date: 02/09/2024

_____
Dean/Principal

Dedicated

to

My Beloved Parents

ACKNOWLEDGEMENTS

Contents

List of Tables

List of Figures

Abstract

In this thesis, main objective to develop reliable and effective numerical methods for solving fractional differential equations. In this work wavelets play a key role in developing numerical methods for solving linear fractional ordinary differential equations with boundary conditions, as well as fractional partial differential equations with both initial and boundary conditions. Also we develop a numerical scheme using operational matrices to solve Caputo and Caputo-Hadamard fractional differential equations. Furthermore, we reproduce a technique called Fast Evaluation, which handles these equations with initial conditions without using operational matrices. A Hadamard-Gegenbauer wavelet method is proposed for the solution of Caputo-Hadamard fractional differential equations. It is applied to solve linear Caputo-Hadamard fractional differential equations for both initial and boundary value problems. Using the Haar wavelet method, we solve fractional ordinary differential equations (ODEs) with initial and boundary value problems. We then present a novel numerical scheme to find approximate solutions for fractional partial differential equations (PDEs). This method combines Haar wavelets with a fast evaluation technique, known as the fast Haar wavelet method. To demonstrate the applicability and accuracy of the method, we solve several examples of Caputo fractional partial differential equations.

Chapter 1

Introduction

The differential calculus, which was invented by G. W. Leibniz and Newton, is the source of fractional calculus, which is equally as old as classical calculus. For the first time, the nth order derivative symbol $\frac{d^n}{dx^n}$ was introduced by G. W. Leibniz. How does this operator function if n is $\frac{1}{2}$, L'Hospital questioned Leibniz. This question inspired S. F. Lacroix, who used the gamma function in his well-known book,to give the formula for the arbitrary order derivative [2]. Lacroix's formula is $\frac{\Gamma(\kappa+1)}{\Gamma(\kappa-\gamma+1)}x^{\kappa-\gamma}$ for the γ order derivative for x^κ. Joseph Liouville extended integer order derivative to fractional order γ. $D^\gamma x^{-\kappa} = (-1)^\kappa \frac{\Gamma(\gamma+\kappa)}{\Gamma(\kappa)} x^{-\gamma-\kappa}$ is the additional formula Liouville developed to expand on his initial definition for fractional order derivative for $\kappa > 0$. The definition only applicable on rational functions. Lacroix's definition is supported by Peacock, while Liouville's is preferred by the majority of scientists. A function's integral representation and its derivatives were obtained by J. Fourier in order to avoid this conflict. Using Liouville's original formulation, Greer developed the fractional derivative for trigonometric and hyperbolic functions. In the 20th century, a number of mathematicians, published a great deal of research on fractional integral and derivative[3, 4].

The philosophy and evolution of fractional calculus have been covered in a number of books [5, 6, 7, 8]. The fractional derivative is introduced via the fractional integral in fractional calculus. Several scholars [5, 6, 7, 8], have been researching and writing a lot on these applications. A novel kind of fractional integral operator, recently presented by multiple mathematicians into a single form[9, 10]. The fractional calculus is now a necessary ingredient in many science and engineering recipes. The fundamental value of fractional calculus is in its ability to be a tool with improved accuracy and to produce exact conclusions in a variety of contexts. The fractional calculus has the unique advantage that these fractional differential operators are no longer local. Thus, the topic considers both non-local dispersed effects and history [11, 12, 13]. The core of fractional differential equations is found in a number of physical issues [14, 15, 16, 17]. Many scholars have been working hard lately to discover strategies and approaches for solving equations for practically useful applications. Researchers are investigating situations that exhibit fractional order behavior on a daily basis. Fractional calculus has essentially been used for simulating heat transfer in heterogeneous media [18], fluid dynamics [19], bioengineering [20] and electromagnetism [21].

We will go over a few essential definitions and special features for your convenience. These are some fractional calculus preliminary notes that will help with future chapters.

1.1 Gamma function

A sort of special function, the gamma function (represented by the Greek sign Γ) is essential to fractional calculus. The expanding of factorial appears to have been originally considered in the 1720s by Daniel Bernoulli and Christian Goldbach. Function, which was initially exclusively defined for positive integers, to the parameters that are non-negative integers. A later discovery of the "Gamma function" was given by Leonhard Euler in 1729 using an integral form with an extended domain that included both real and complex values in addition to positive integers. It was researched by numerous mathematicians after Euler in order to improve the expression of the gamma function. For each positive number p, Gamma function is defined as

$$\Gamma(p) = (p-1)!$$

Definition 1.1.1. [22] The function $\Gamma : (0, \infty) \to \mathbb{R}$, is defined by,

$$\Gamma(p) = \int_0^\infty s^{p-1} e^{-s} ds.$$

Euler's Gamma function, and for $p \in \mathbb{R}^+$, the above improper integral converges. The gamma function has a wide range of features, some of which we will address below.

1.1.1 Properties of Euler's Gamma Function

1. $\Gamma(p) = (p-1)\Gamma(p-1)$,   for all $p > 1$,

Proof. According to the definition of gamma function,

$$\Gamma(p) = \int_0^\infty s^{p-1} e^{-s} ds,$$

by parts integration of above equation yields

$$\Gamma(p) = \left\{ -s^{p-1} e^{-s} \right\}_0^\infty + \int_0^\infty (p-1) s^{p-2} e^{-s} ds,$$

$$= 0 + \int_0^\infty (p-1) s^{p-2} e^{-s} ds,$$

$$= (p-1) \int_0^\infty s^{p-2} e^{-s} ds,$$

$$= (p-1)\Gamma(p-1),$$

If p is an integer, $p = 1, 2, 3, \ldots$, then,

$$\Gamma(p) = (p-1)\Gamma(p-1),$$
$$= (p-1)(p-2)\Gamma(p-2),$$
$$= (p-1)(p-2)(p-3)\Gamma(p-3),$$
$$= (p-1)(p-2)(p-3), \ldots, 1,$$
$$= (p-1)!.$$

Therefore, for a positive integer argument the gamma function can be reduced into factorial function.

1.1.2 Extension of Gamma Function's Domain

Domain of gamma function can be extended, we rewrite equation,

$\Gamma(p) = (p-1)\Gamma(p-1)$, as [22],

$$\Gamma(p+1) = (p)\Gamma(p), \quad \text{for } p > 0$$
$$\Gamma(p) = \frac{\Gamma(p+1)}{p}. \tag{1.1}$$

For $p + 1 > 0, p > -1, p \neq 0$, function on right hand side is defined. Now from equation (1.1),

$$\Gamma(p+2) = (p+1)p\Gamma(p),$$
$$\Gamma(p) = \frac{\Gamma(p+2)}{p(p+1)}.$$

After repeating the above process m-times, we get,

$$\Gamma(p) = \frac{\Gamma(p+m)}{p(p+1)(p+2)(p+3), \ldots, (p+m-1)}, \quad m \neq 0, -1, -2, \cdots,$$

1.2 Riemann-Liouville Integral

The integral formula of Cauchy is used to define fractional integrals and derivatives.

$$_x\mathbb{I}_a^n \Phi(x) = \int_a^x \frac{(x-\tau)^{n-1}\Phi(\tau)}{(n-1)!} d\tau, \tag{1.2}$$

where $n \in \mathbb{N}$, and $\Phi \in L_1[a,b], a, b \in \mathbb{R}$.
The definition of fractional integral is obtained by changing the factorial in (1.2) to the gamma function.

Definition 1.1.2 [23] The fractional integral of Riemann-Liouville of order γ is defined as, let $\gamma \in \mathbb{R}^+$, and the operator $_x\mathbb{I}_a^\gamma$, defined on $L_1[a,b]$ by,

$$\left(_x\mathbb{I}_a^\gamma \Phi \right)(x) = \frac{1}{\Gamma(\gamma)} \int_a^x (x-\tau)^{\gamma-1}\Phi(\tau)d\tau, \tag{1.3}$$

for $a \leq x \leq b$, the operator $_x\mathbb{I}_a^\gamma$ is known as the fractional integral operator of Riemann-Liouville or precisely R - L operator.
For $\gamma = 0$, we have $_x\mathbb{I}_a^0 \Phi = \Phi$ which is the identity operator, if $\gamma \in \mathbb{N}$, then $_x\mathbb{I}_a^\gamma \Phi$ coincides with the classical integral.

1.2.1 Riemann-Liouville Derivative

We discuss the concepts that lead the definition of the fractional differential operator. The fundamental theorem of integer order calculus yields $_x\mathbb{D}_a^n {_x}\mathbb{I}_a^n \Phi = \Phi$, where $n \in \mathbb{N}$ denotes the order of the

differential and integral operators. For $n_1, n_2 \in \mathbb{N}$, we can alternatively write ${}_x\mathbb{D}_a^{n_1-n_2}{}_x\mathbb{I}_a^{n_1-n_2}\Phi = \Phi$. Consequently, we may write,

$$ {}_x\mathbb{D}_a^{n_2}\Phi = {}_x\mathbb{D}_a^{n_1}{}_x\mathbb{I}^{n_1-n_2}\Phi. \tag{1.4} $$

Relation (1.4) holds true for a certain class of functions if n_2 is replaced with any $\gamma > 0$, unless $n_1 - n_2 > 0$. The Riemann-Liouville fractional definition of differential operator follows from this.

Definition 1.1.3. [23] For $\gamma \in \mathbb{R}^+$ Considering $\gamma \in \mathbb{R}^+$, The fractional derivative of Riemann-Liouville is;

$$ {}_x\mathbb{D}_a^\gamma \Phi(x) = \frac{1}{\Gamma(n-\gamma)}\left(\frac{d}{dx}\right)^n \int_a^x (x-\tau)^{n-\gamma-1}\Phi(\tau)d\tau, \tag{1.5} $$

where $n - 1 < \gamma \leq n$.

1.3   Caputo Fractional Order Derivative

Caputo used the definition of fractional integral to define fractional derivative.

Definition 1.1.4[1] If $f : \mathbb{R}_+ \to \mathbb{R}$ and $\gamma \in \langle n-1, n\rangle, n \in \mathbb{N}$, then,

$$ {}_x^C D_0^\gamma \Phi(x) = \frac{1}{\Gamma(n-\gamma)} \int_0^x \frac{\Phi^{(n)}(\tau)}{(x-\tau)^{\gamma-n+1}}d\tau, \tag{1.6} $$

where the gamma function is represented by Γ, is called the Caputo fractional derivative of order γ, provided it exists.

According to Caputo, the integral of Riemann-Liouville of fractional order is found by first computing the ordinary derivative of natural order and then using the function that is obtained to define the fractional order derivative. For $\gamma \in \langle n-1, n\rangle, {}_x^C D_0^\gamma \Phi(x)$, then $\Phi \in C^n(\langle 0, x\rangle)$ if and only if. The Caputo fractional derivative is a non-local operator as it is defined in integral form.

Theorem 1.1.5.[1] The Caputo derivative is a linear operator, i.e. for any $a, b \in \mathbb{R}$,

$$ {}_x^C D_0^\gamma(a\Phi_1(x) + b\Phi_2(x)) = a{}_x^C D_0^\gamma \Phi_1(x) + b{}_x^C D_0^\gamma \Phi_2(x), $$

Proof. Let ${}_x^C D_0^\gamma \Phi_1(x), {}_x^C D_0^\gamma \Phi_2(x)$ be the Caputo derivatives of functions Φ_1 and Φ_2, respectively. Then

$$ {}_x^C D_0^\gamma(a\Phi_1(x) + b\Phi_2(x)) = \frac{1}{\Gamma(n-\gamma)} \int_0^x \frac{(a\Phi_1(x) + b\Phi_2(x))^{(n)}}{(x-\tau)^{\gamma-n+1}}d\tau, $$

$$ = \frac{1}{\Gamma(n-\gamma)}\left(a\int_0^x \frac{\Phi_1^{(n)}(x)}{(x-\tau)^{\gamma-n+1}}d\tau + b\int_0^x \frac{\Phi_2^{(n)}(x)}{(x-\tau)^{\gamma-n+1}}d\tau\right), $$

$$ = \frac{1}{\Gamma(n-\gamma)}a\int_0^x \frac{\Phi_1^{(n)}(x)}{(x-\tau)^{\gamma-n+1}}d\tau + \frac{1}{\Gamma(n-\gamma)}b\int_0^x \frac{\Phi_2^{(n)}(x)}{(x-\tau)^{\gamma-n+1}}d\tau, $$

$$= a_x^C D_0^\gamma \Phi_1(x) + b_x^C D_0^\gamma \Phi_2(x).$$

Theorem 1.1.6.[25] The Caputo fractional derivative of the order $\gamma = 0$ for Φ is equal to Φ, i.e. $_x^C D_0^\gamma \Phi(x) = \Phi(x)$.

Proof. For any Φ, let the Caputo derivative of order $\gamma = 0$ exist. $n = 1$ as a result, and from (1.3.1) it follows,

$$_x^C D_0^\gamma \Phi(x) = \frac{1}{\Gamma(1)} \int_0^x \frac{\Phi'(\tau)}{(x-\tau)^{-1+1}} d\tau = \int_0^x \Phi'(\tau) d\tau = \Phi(x).$$

Theorem 1.1.7.[24] For the Caputo derivative of arbitrary order, the index law is valid, i.e.

$$_x^C D_0^{\gamma}{}_x^C D_0^\beta \Phi(x) =_x^C D_0^{\gamma+\beta} \Phi(x),$$

for any $\gamma, \beta \in \langle n-1, n), n \in \mathbb{N}$.
Alternatively known as the semigroup property of the Caputo fractional operator $_x^C D_0^\gamma$.

1.4   Hadamard Fractional Integral and Derivative

The Hadamard fractional integral was introduced in 1892 by Jacques Hadamard and stated as
Definition 1.1.8.[26] For $\gamma \in \mathbb{R}^+$ and the function $f(\tau) \in L^p[a,b]$. Then the Hadamard fractional integral operator is defined as,

$$\left(_x\mathbb{I}_a^\gamma \Phi\right)(x) = \frac{1}{\Gamma(\gamma)} \int_a^x \left(\ln \frac{x}{\tau}\right)^{\gamma-1} \Phi(\tau) \frac{d\tau}{\tau}, \quad x > a, \tag{1.7}$$

and if $\Phi(x) \in AC^n[a,b]$ then the Hadamard derivative is introduced as

$$\left(_x^H \mathbb{D}_a^\gamma \Phi\right)(x) = \frac{1}{\Gamma(n-\gamma)} \left(x\frac{d}{dx}\right)^n \int_a^x \left(\ln \frac{x}{\tau}\right)^{n-\gamma-1} \Phi(\tau)\frac{d\tau}{\tau}, \quad x > a. \tag{1.8}$$

1.5   Wavelets

Joseph Fourier, a French mathematician has been discovered that the complex functions may be approximated and represented as a weighted sun of fundamental trigonometric functions in 1807. Such approximations and representations have a number of advantages, since they offer comprehensive analysis of complex functions. Fourier transformation is a powerful tool for data analysis, which uses sinusoidal waves as basis functions. However, forever oscillation of sinusoidal waves obstructs the

representation of abrupt changes efficiently. Moreover, sinusoids are not localized in time domain, instead they are perfectly localized in frequency domain which is the major drawback of sinusoidal representation. Therefore, non-stationary signals cannot be approximated by Fourier transformation. Consequently, the analysis of images and non-stationary signals require a representation in which functions are well localized in not only time but also in frequency domain. The modification of Fourier transform into short time Fourier transform was firstly presented by Dennis Gabor in 1946 [27]. Short time Fourier transform sectioned a signal to a time-localized window and for every window section of signal, Fourier transform was computed. It had a major flaw that the analysis of entire signal through the fixed width of window function resulted in a fixed resolution. Jean Morlet, in 1982, was firstly presented the idea of utilizing distinct window function for distinct frequency bands, generating by scaling and shifting of a single window function in time-frequency domain. Morlet referred these basis functions as wavelets of constant shape because the window functions are tiny and oscillatory by nature.

Wavelets are special types of compactly supported oscillatory functions that act as the foundation for numerous significant spaces. These functions exhibit oscillatory behaviour for a short time period and then die out. They has been used to solve various problems in the field of science and engineering. Several specific properties of wavelets make them very useful [28]. Wavelets are frequently used in numerical analysis [29], signal analysis for waveform representation and segmentation [30], system analysis, optimal control and time-frequency analysis [31]. Recently, wavelet methods for solving differential and integral equations have been getting more attention. Differential equations were first solved using Haar wavelets and Legendre wavelets in [32] and [33] respectively.

Wavelets are formed by a family of functions which are constructed from translation and dilation of a single function, known as mother wavelet $\phi(s)$. A family of continuous functions where the translation parameter b and the dilation parameter a vary continuously, defined as

$$\phi_{a,b}(s) = |a|^{-\frac{1}{2}} \phi\left(\frac{s-b}{a}\right), a, b \in \mathbb{R}, a \neq 0. \tag{1.9}$$

The wavelet compresses by taking $|a| < 1$ with small support in time domain and higher support in frequency domain. On the contrary, when $|a| > 1$ the wavelet expands and has less support in the frequency domain along with greater support in the time domain. By restricting the parameters as $a = \gamma_0^{-k}$ and $b = n\gamma_1\gamma_0^{-k}, \gamma_0, \gamma_1 > 0$ for $n, k \in \mathbb{Z}^+$, following family of discrete wavelets is obtained [34]

$$\phi_{k,n}(s) = |\gamma_0|^{\frac{k}{2}} \phi\left(\gamma_0^k s - n\gamma_1\right). \tag{1.10}$$

In the above equation $\phi_{k,n}(s)$, forms a wavelet basis of $L^2(\mathbb{R})$.

1.5.1 Types of Wavelets Transforms

There are two different kinds of wavelet transforms discrete and continuous. Wavelet transformations are used to transform a signal from the time domain to the time-frequency domain through Wavelets.

Continuous Wavelet Transform

Let $g(s) \in L^2(\mathbb{R})$ and the mother wavelet $\phi_{a,b}(s) \in L^2(\mathbb{R})$, then the continuous wavelet transform [28] is defined as

$$CWT_g(a,b) = |a|^{-\frac{1}{2}} \int_{-\infty}^{\infty} g(s)\phi\left(\frac{s-b}{a}\right), \tag{1.11}$$

where $|a|^{-\frac{1}{2}}$ is normalization factor. Time frequency analysis and filtering of frequency components in localized time are basic applications of continuous wavelets transforms (CWT). Since, the analytical wavelets have non negative frequency components, they are best suited wavelets for time frequency analysis. Analytical Morlet wavelet, Bump wavelets and Morse wavelet are some of the examples that are adapted for continuous wavelet analysis [35]. The output of CWT appears in the form of coefficients that are functions of time and frequency. By using CWT the oscillatory behaviour of signals is characterized adequately.

Discrete Wavelet Transform

Since the function $g(s)$ and the wavelet $\phi\left(\frac{s-b}{a}\right)$ are correlated in continuous wavelets transform while the wavelet is translated and scaled, hence the continuous wavelet transform (CWT) is not more practicable. Infinitely many unessential coefficients in CWT are obtained during calculations, therefore discretization is performed. Furthermore, continuous wavelet transforms mainly use wavelet functions, whereas discrete wavelet transforms use scaling and wavelet functions simultaneously. Discrete wavelet transform is an ideal case of denoising and compressing of naturally occurring signals and images without redundant coefficients. The continuous representation of a function in (1.5.1) may turned into discrete form by considering only integer values of a and b. Discrete wavelet transform can be described by setting $a = 2^{-j}$ and $b = k2^{-j}$, defining j as the refinement level and k controls the shifting of wavelet being an integer variable [28].

$$\phi_{j,k}(s) = |a|^{\frac{j}{2}}\phi\left(2^j s - k\right). \tag{1.12}$$

These wavelets for $j,k = 1,2,\cdots$, generate an orthogonal basis, referred to the mother wavelet. Through translation and dilation of mother wavelet further wavelets can be generated. Discretization of wavelets based on scaling and translation, along with unaltered time domain. The basic applications of discrete wavelet analysis are denoising and scaling the images and signals. We will further discuss some important properties and types of wavelets in this section.

1.5.2 Properties of Wavelets

There are many important properties of wavelets, some of which are described here.

Admissibility

The admissibility and regularity conditions have been considered the most important properties of wavelets, by which different wavelets are distinguished. For a wavelet ϕ the admissibility condition is defined as [36]

$$\mathcal{A}_\phi = \int_{-\infty}^{+\infty} \frac{|\zeta(x)|^2}{|x|} dx < +\infty, \tag{1.13}$$

where $\zeta(x)$ is the Fourier transform of $\phi(s)$. According to the admissibility condition, $\zeta(x)$ vanishes quickly as $x \to 0$, i-e;

$$\zeta(0) = \int_{-\infty}^{+\infty} \zeta(x)dx = 0.$$

Regularity Condition

The wavelet transform's time-bandwidth product is the square of the input signal, which is undesirable in most practical applications. As a result, some extra constraints are imposed on the wavelet functions to make the wavelet transform shrink rapidly with decreasing scale a. The regularity criteria imply that the wavelet function should be smooth and concentrated in both the frequency and temporal domains. We can explain regularity by using the concept of vanishing moments. The vanishing moment is a criterion for determining how a function $g(s)$ decays to infinity. Using the integration below, we can compute the decay rate,

$$\left[\int_{-\infty}^{\infty} s^q g(s)ds \right] = 0, \tag{1.14}$$

where q is the decay rate. Also if a wavelet $\phi(s)$ has N vanishing moments, then the wavelet transform's approximation order is also N. Through a number of vanishing moments, one can discuss the regularity of wavelets. A wavelet with more vanishing moments will be considered more regular.

Multiresolution Analysis

There exists a finite number of wavelet coefficients in any discretized wavelet transform for a given enclosed rectangular area in the plane's upper half. Nevertheless, each coefficient involves the calculation of an integral. This numerical complexity can be eliminated under certain cases if the wavelets constitute a multiresolution analysis. The multiresolution signal analysis is performed by wavelet transform, through the varying scale factor a. In account to process the signal differently and independently in each frequency band, the multiresolution signal analysis decomposes the signal into numerous frequency bands. Therefore, the wavelet must be localized in the timefrequency domain [37].

Linear Transform Property

Wavelet transform is a linear operation according to its definition. For a given function $g(s)$, its wavelet transform $\phi_g(a, b)$ has the following property

$$\phi_{g_1 + g_2}(a, b) = \phi_{g_1}(a, b) + \phi_{g_2}(a, b).$$

For translation and scaling parameters, we have

$$\phi_{g(b-b_0)}(a, b) = \phi_{g(s)}(a, b - b_0),$$

$$\phi_{\beta^{\frac{1}{2}} g(\beta s)}(a, b) = \phi_{g(s)}(\beta a, \beta b).$$

For $g(s) = C$, where C is any constant function, by admissibility condition its wavelet transform is zero.

1.5.3   Some Famous Wavelets

There are various kinds of wavelets, out of which some famous wavelets are mentioned below. Daubechies was the first to proposed compactly supported wavelets with orthonormal bases for $L^2(\mathbb{R})$ space in 1988. These wavelets follow the Galerkin approach to discretize the differential equation and possess various desirable properties, such as compact support, orthogonality, an exact representation of polynomials to a certain extent, and the capability to express functions at multiple resolution levels. But due to lack of an explicit expression in Daubechies' wavelets, they were not efficient to provide analytical differentiation or integration.

Haar Wavelets

The Haar wavelets proposed in 1909 by Alfred Haar, serves as the basic orthonormal wavelet with compact support. On the interval of $[0, 1)$, family of Haar wavelets is defined as [38]

$$\mathcal{H}_i(s) = \begin{cases} 1, & \beta_1 \le s < \beta_2, \\ -1, & \beta_2 \le s < \beta_3, \\ 0, & \text{elsewhere}, \end{cases} \tag{1.15}$$

where $\beta_1 = \frac{k}{m}, \beta_2 = \frac{k+0.5}{m}, \beta_3 = \frac{k+1}{m}$. In the above definition $i = 2^j + k + 1, j = 1, 2, \cdots, J$ is the scaling parameter, where J is maximum resolution level. Also $m = 2^j$ and $k = 1, 2, \cdots, m - 1$, is translation parameter. In 1980s, it was found that, Haar wavelets are in fact the first order Daubechies wavelet and known as Db1. The Haar wavelets are further divided into two categories i-e; Uniform Haar wavelets and Non-Uniform Haar wavelets bases on wavelet's behaviour [39]. The major drawback of Haar wavelets is that they disobey continuity as well as differentiability.

Legendre Wavelets

These wavelets are compactly supported and derived from orthogonal Legendre polynomials through translation and expansion. Legendre wavelets with respect to the independent variable s are defined on $[0, 1]$, as [42]

$$\phi_{k,n}^l(s) = \begin{cases} \sqrt{l + \frac{1}{2}} 2^{\frac{k}{2}} P_l\left(2^k s - 2n + 1\right), & \frac{2n-2}{2^k} \le s < \frac{2n}{2^k}, \\ 0, & \text{elsewhere}, \end{cases} \tag{1.16}$$

where $m = 1, 2, \cdots, 2n-1$, is the Legendre polynomials' order, $n = 1, 2, \cdots, 2^{k-1}$, $k \in \mathbb{Z}^+$, and $\sqrt{l + \frac{1}{2}}$ is the factor of standardization. These wavelets are also referred as spherical harmonic wavelets. The Legendre wavelets use linear phase finite impulse response (FIR) filter during multiresolution analysis, which enhance their uses in various physical phenomenons. Legendre wavelets have been used to address fractional delay differential equations numerically in [40], and also used to inspect heat transfer and Unsteady flow of tangent-hyperbolic fluid in [41].

Chebychev Wavelets

The Chebychev wavelets are defined over the interval $[0, 1)$, as,

$$
\phi_{n,m}(s) = \begin{cases} 2^{\frac{k}{2}} \tilde{\Theta}_m \left(2^k s - 2n + 1\right), & \frac{\hat{n}-1}{2^k} \le s < \frac{\hat{n}}{2^k}, \\ 0, & \text{elsewhere,} \end{cases} \tag{1.17}
$$

where

$$
\tilde{\Theta}_m(s) = \begin{cases} \frac{1}{\sqrt{\pi}}, & m = 0, \\ \sqrt{\frac{2}{\pi}} \Theta_m(s), & m > 0, \end{cases} \tag{1.18}
$$

and $m = 0, 1, 2, \ldots, M-1$, $k = 1, 2, \ldots, 2^{k-1}$, where M and k are positive integers. Chebyshev wavelets utilize shifted Chebyshev polynomials $\tilde{\Theta}_m(s)$, transforming the domain of Chebyshev polynomials $\theta_m(s)$ from $[-1, 1]$ to $[0, 1]$. Chebyshev polynomials are also orthogonal polynomials and have gained popularity in approximation theory. The all four types of Chebyshev polynomials are special cases of Jacobi polynomials. Some recent applications of Chebychev wavelets in the field of medical science is presented in [43].

Chapter 2

Fast Evaluation Technique

In recent years, fast evaluation techniques for Caputo and Caputo-Hadamard fractional differential equations have become very important for solving complex mathematical problems. These methods help solve the problems caused by fractional derivatives, which are difficult to compute because they depend on the entire history of the solution. For the Caputo fractional derivative, which is often used to model processes with memory effects, there have been significant improvements with fast finite difference methods. Jiang et al.[44] have developed stable, fast time-stepping methods that make handling these operators more efficient, especially in applications like fractional diffusion equations. These advancements make it easier to simulate processes such as diffusion, which are important in various scientific and engineering fields. For Caputo-Hadamard fractional differential equations, new numerical methods have also been developed to improve computational efficiency. The Caputo-Hadamard derivative, combining features of the Caputo and Hadamard derivatives, is particularly useful for initial value problems. Methods like the predictor-corrector approach, which use graded and non-uniform meshes, have shown great promise in achieving optimal convergence even under weak smoothness conditions. Green et al.[50] have shown the effectiveness of these methods through numerical experiments, demonstrating significant performance improvements. Moreover, Gohar et al.[43] have developed finite difference methods specifically for Caputo-Hadamard fractional differential equations, further improving computational efficiency.

Overall, these advances in fast evaluation techniques help us better understand fractional differential equations. They also expand the practical uses of fractional differential equations in fields like physics, engineering, and applied mathematics. The methods and insights from these studies are important for developing more efficient and accurate solutions for these complex equations.

2.1 Fast Evaluation Technique of Caputo Fractional Derivative of Order γ

In this section, we will consider one of the fast evaluation techniques, to solve the Caputo fractional derivative for $0 < \gamma < 1$. Suppose we want to evaluate the Caputo fractional derivative on the interval $[0, T]$ over a set of grid points $\Omega_\zeta := \{\zeta_n, n = 0, 1, \cdots, N_T\}$, with $\zeta_0 = 0$, $\zeta_{N_T} = T$, and $\Delta\zeta_n = \zeta_n - \zeta_{n-1}$.

Caputo fractional derivative defined as,

$$\left. {}_\zeta^C D_0^\gamma y(\zeta) \right|_{\zeta=\zeta_n} = \frac{1}{\Gamma(1-\gamma)} \int_0^{\zeta_n} \frac{y'(s)ds}{(\zeta_n - s)^\gamma}. \tag{2.1}$$

Splitting the convolution integral (2.1) into two components: a local part and a history part.

$$= \frac{1}{\Gamma(1-\gamma)} \int_{\zeta_{n-1}}^{\zeta_n} \frac{y'(s)ds}{(\zeta_n - s)^\gamma} + \frac{1}{\Gamma(1-\gamma)} \int_0^{\zeta_{n-1}} \frac{y'(s)ds}{(\zeta_n - s)^\gamma},$$

$$\left. {}^C_\zeta D_0^\gamma y(\zeta) \right|_{\zeta=\zeta_n} := L\left(\zeta_n\right) + H\left(\zeta_n\right), \tag{2.2}$$

where $L_n = \frac{1}{\Gamma(1-\gamma)} \int_{\zeta_{n-1}}^{\zeta_n} \frac{y'(s)ds}{(\zeta_n-s)^\gamma}$ and $H_n = \frac{1}{\Gamma(1-\gamma)} \int_0^{\zeta_{n-1}} \frac{y'(s)ds}{(\zeta_n-s)^\gamma}$, are history and local parts, respectively. For the local part, we approximate $y'(s)$ by a constant $\frac{y(\zeta_n)-y(\zeta_{n-1})}{\Delta\zeta_n}$ to get,

$$L\left(\zeta_n\right) \approx \frac{1}{\Gamma(1-\gamma)} \int_{\zeta_{n-1}}^{\zeta_n} \left(\zeta_n - s\right)^{-\gamma} \left[\frac{y\left(\zeta_n\right) - y\left(\zeta_{n-1}\right)}{\Delta\zeta_n} \right] ds.$$

As the result,

$$L\left(\zeta_n\right) \approx \frac{1}{\Gamma(1-\gamma)} \left[\frac{y\left(\zeta_n\right) - y\left(\zeta_{n-1}\right)}{\Delta\zeta_n} \right] \int_{\zeta_{n-1}}^{u_n} \left(\zeta_n - s\right)^{-\gamma} ds,$$

$$L\left(\zeta_n\right) \approx \frac{1}{\Gamma(2-\gamma)} \left[\frac{y\left(\zeta_n\right) - y\left(\zeta_{n-1}\right)}{(\Delta\zeta_n)^\gamma} \right]. \tag{2.3}$$

Now for calculating the history part, we employ the integration by parts to substitute $y'(s)$ and obtain.

$$H(\zeta_n) = \frac{1}{\Gamma(1-\gamma)} \int_0^{\zeta_{n-1}} \frac{y'(s)ds}{(\zeta_n - s)^\gamma},$$

$$H\left(\zeta_n\right) = \frac{1}{\Gamma(1-\gamma)} \left[\frac{y\left(\zeta_{n-1}\right)}{(\Delta\zeta_n)^\gamma} - \frac{y\left(\zeta_0\right)}{(\zeta_n)^\gamma} - \gamma \int_0^{\zeta_{n-1}} \frac{y(s)}{(\zeta_n - s)^\gamma} ds \right]. \tag{2.4}$$

To formulate efficient sum-of-exponentials(SOE)[46], we will use the approximations for the kernel $\zeta^{-\alpha}(0 < \alpha < 2)$ on the interval $[\delta, T]$ with $\delta = \min_{1 \leq n \leq N} \Delta\zeta_n$ and the absolute error ϵ. There exist positive real numbers s_i and ω_i $(i = 1, \ldots, N_{\exp})$ such that for $0 < \alpha < 2$.

$$\left| \frac{1}{\zeta^\alpha} - \sum_{i=1}^{N_{exp}} \omega_i e^{-s_i \zeta} \right| \leq \epsilon, \quad \zeta \in [\delta, T], \tag{2.5}$$

where the order of N_{exp} defined as,

$$N_{\exp} = \mathcal{O} \left(\log \frac{1}{\epsilon} \left(\log\log \frac{1}{\epsilon} + \log \frac{T}{\delta} \right) + \log \frac{1}{\delta} \left(\log\log \frac{1}{\epsilon} + \log \frac{T}{\delta} \right) \right). \tag{2.6}$$

Lemma 2.1.1. For $\alpha > 0$,

$$\frac{1}{\zeta^\alpha} = \frac{1}{\Gamma(\alpha)} \int_0^\infty e^{-\zeta \cdot s} s^{\alpha-1} ds. \tag{2.7}$$

Lemma 2.1.2. For $\zeta \geq \alpha > 0$,

$$\left| \frac{1}{\Gamma(\alpha)} \int_p^\infty e^{-\zeta s} s^{\alpha-1} ds \right| \leq \begin{cases} e^{-\delta p} \frac{p^{\alpha-1}}{\Gamma(\alpha)} \frac{1}{\delta}, & 0 < \alpha \leq 1, \\ e^{-\delta p} 2^{\alpha-1} \left(\frac{p^\alpha}{\Gamma(\alpha)} + \frac{1}{\delta^\alpha} \right), & 1 < \alpha < 2. \end{cases} \tag{2.8}$$

13

To approximate the history part (2.4), we will modify the convolution kernel $\zeta^{-1-\gamma}$ with SOE.

$$H\left(\zeta_n\right) \approx \frac{1}{\Gamma(1-\gamma)}\left[\frac{y\left(\zeta_{n-1}\right)}{\left(\Delta\zeta_n\right)^\gamma} - \frac{y\left(\zeta_0\right)}{\left(\zeta_n\right)^\gamma} - \gamma\sum_{i=1}^{Nexp} w_i \int_0^{\zeta_{n-1}} e^{-(\zeta_n-s)s_i}y(s)ds\right], \tag{2.9}$$

$$H\left(\zeta_n\right) = \frac{1}{\Gamma(1-\gamma)}\left[\frac{y\left(\zeta_{n-1}\right)}{\left(\Delta\zeta_n\right)^\gamma} - \frac{y\left(\zeta_0\right)}{\left(\zeta_n\right)^\gamma} - \gamma\sum_{i=1}^{Nexp} w_i y_{hist,i}\left(\zeta_n\right)\right]. \tag{2.10}$$

The new function $y_{hist,i}\left(\zeta_n\right)$ introduced as,

$$y_{hist,i}\left(\zeta_n\right) = \int_0^{\zeta_{n-1}} e^{-(\zeta_n-s)s_i}y(s)ds. \tag{2.11}$$

For $n = 1, 2, \ldots, N_T$, this forms a recurrence relation:

$$y_{hist,i}\left(\zeta_n\right) = \int_0^{\zeta_{n-2}} e^{-(\zeta_n-s)s_i}y(s)ds + \int_{\zeta_{n-2}}^{\zeta_{n-1}} e^{-(\zeta_n-s)s_i}y(s)ds. \tag{2.12}$$

By utilizing equation (2.11), we will obtain a simplified expression.

$$y_{hist,i}\left(\zeta_n\right) = e^{-(si\Delta\zeta_n)}y_{hist,i}\left(\zeta_{n-1}\right) + \int_{\zeta_{n-2}}^{\zeta_{n-1}} e^{-(\zeta_n-s)s_i}y(s)ds, \tag{2.13}$$

where

$$\int_{\zeta_{n-2}}^{\zeta_{n-1}} e^{-(\zeta_n-s)s_i}y(s)ds = \frac{e^{-(si\Delta\zeta_n)}}{si^2\Delta\zeta_{n-1}}\left[\left(e^{-si\Delta\zeta_{n-1}} - 1 + si\Delta\zeta_{n-1}\right)y\left(\zeta_{n-1}\right) + \right.$$
$$\left.\left(1 - e^{-si\Delta\zeta_{n-1}} - e^{-si\Delta\zeta_{n-1}}si\Delta\zeta_{n-1}\right)y\left(\zeta_{n-2}\right)\right]. \tag{2.14}$$

By applying equation (2.14) within equation (2.13), we obtain

$$y_{hist,i}\left(\zeta_n\right) = e^{-(si\Delta\zeta_n)}y_{hist,i}\left(\zeta_{n-1}\right) + \frac{e^{-(si\Delta\zeta_n)}}{si^2\Delta\zeta_{n-1}}\left[\left(e^{-si\Delta\zeta_{n-1}} - 1 + si\Delta\zeta_{n-1}\right)y\left(\zeta_{n-1}\right) + \right.$$
$$\left.\left(1 - e^{-si\Delta\zeta_{n-1}} - e^{-si\Delta\zeta_{n-1}}si\Delta\zeta_{n-1}\right)y\left(\zeta_{n-2}\right)\right]. \tag{2.15}$$

Obtaining the history part by applying equation (2.15) to equation (2.10),

$$H_n\left(\zeta_n\right) \approx \frac{1}{\Gamma(1-\gamma)}\left[\frac{y\left(\zeta_{n-1}\right)}{\left(\Delta\zeta_n\right)^\gamma} - \frac{y\left(\zeta_0\right)}{\left(\zeta_n\right)^\gamma} - \gamma\sum_{i=1}^{Nexp} w_i \left(e^{-(si\Delta\zeta_n)}y_{hist,i}\left(\zeta_{n-1}\right) + \frac{e^{-(si\Delta\zeta_n)}}{si^2\Delta\zeta_{n-1}}\right.\right.$$
$$\left.\left.\left[(e^{-si\Delta\zeta_{n-1}} - 1 + si\Delta\zeta_{n-1})y(\zeta_{n-1}) + \left(1 - e^{-si\Delta\zeta_{n-1}} - e^{-si\Delta\zeta_{n-1}}si\Delta\zeta_{n-1}\right)y\left(\zeta_{n-2}\right)\right]\right)\right]. \tag{2.16}$$

Through the combination of equations (2.3) and (2.16), we achieve a Fast evaluation technique for

the Caputo fractional derivative.

$$
\begin{aligned}
{}^{C}_{0}D^{\gamma}_{\zeta}y(\zeta_n) \approx & \frac{1}{\Gamma(2-\gamma)} \left[\frac{y(\zeta_n) - y(\zeta_{n-1})}{(\Delta\zeta_n)^{\gamma}} \right] + \frac{1}{\Gamma(1-\gamma)} \left[\frac{y(\zeta_{n-1})}{(\Delta\zeta_n)^{\gamma}} - \frac{y(\zeta_0)}{(\zeta_n)^{\gamma}} \right. \\
& -\gamma \sum_{i=1}^{N_{exp}} w_i \left(e^{-(s_i\Delta\zeta_n)} y_{hist,i}(\zeta_{n-1}) + \frac{e^{-(s_i\Delta\zeta_n)}}{s_i^2\Delta\zeta_{n-1}} \left[(e^{-s_i\Delta\zeta_{n-1}} - 1 \right. \right. \\
& \left. \left. \left. +s_i\Delta\zeta_{n-1})y(\zeta_{n-1}) + \left(1 - e^{-s_i\Delta\zeta_{n-1}} - e^{-s_i\Delta\zeta_{n-1}} s_i\Delta\zeta_{n-1} \right) y(\zeta_{n-2}) \right] \right) \right] .
\end{aligned}
\tag{2.17}
$$

Remark. However, we will continue to use a uniform temporal mesh with equal intervals, denoted as $\Delta\zeta_n = \Delta\zeta$. We have discovered that the Caputo fractional derivative works best for non-uniform meshes.

2.2   Error analysis

Here, we will perform an error analysis of the fast evaluation method. This analysis aims to assess the accuracy and stability of the method in computing the desired values, offering valuable insights into its reliability and effectiveness.

Lemma 2.1.3.[45] Suppose that $y(\zeta) \in C^2[0, \zeta_n]$ and let

$$
{}^{F}R^n y := {}^{C}_{0}D^{\gamma}_{\zeta}y(\zeta)\Big|_{\zeta=\zeta_n} - {}^{FC}_{0}\mathbb{D}^{\gamma}_{\zeta}y^n,
\tag{2.18}
$$

where $0 < \gamma < 1$. Then,

$$
\left| {}^{F}R^n y \right| \leq \frac{\Delta\zeta^{2-\gamma}}{\Gamma(2-\gamma)} \left(\frac{1-\gamma}{12} + \frac{2^{2-\gamma}}{2-\gamma} - (1+2^{-\gamma}) \right) \max_{0\leq\zeta\leq\zeta_n} \left| y''(\zeta) \right| + \frac{\gamma\varepsilon\zeta_{n-1}}{\Gamma(1-\gamma)} \max_{0\leq\zeta\leq\zeta_{n-1}} |y(\zeta)].
\tag{2.19}
$$

Proof. Only difference between our approximation ${}^{FC}_{0}\mathbb{D}^{\gamma}_{\zeta}y^n$ and the L1 approximation ${}^{C}_{0}\mathbb{D}^{\gamma}_{\zeta}y^n$ lies in the convolution kernel's and an absolute error bound of ε in its sum-of-exponentials approximation(2.5).

$$
\left| {}^{FC}_{0}\mathbb{D}^{\gamma}_{\zeta}y^n - {}^{C}_{0}\mathbb{D}^{\gamma}_{\zeta}y^n \right| \leq \frac{\gamma\varepsilon}{\Gamma(1-\gamma)} \sum_{j=1}^{n-1} \int_{\zeta_{j-1}}^{\zeta_j} \left| \Pi_{1,j}y(s) \right| ds,
\tag{2.20}
$$

where $\Pi_{1,j}y(\zeta) = y(\zeta_{j-1})\frac{\zeta_j-\zeta}{\Delta\zeta} + y(\zeta_j)\frac{\zeta-\zeta_{j-1}}{\Delta\zeta}$, and leading the triangle inequality,

$$
\left| {}^{F}R^n y \right| \leq \left| {}^{C}R^n y \right| + \frac{\gamma\varepsilon}{\Gamma(1-\gamma)} \sum_{j=1}^{n-1} \int_{\zeta_{j-1}}^{\zeta_j} \left| \Pi_{1,j}y(s) \right| ds,
\tag{2.21}
$$

where,

$$
\sum_{j=1}^{n-1} \int_{\zeta_{j-1}}^{\zeta_j} \left| \Pi_{1,j}y(s) \right| ds \leq \max_{0\leq\zeta\leq\zeta_{n-1}} |y(\zeta)|\zeta_{n-1}.
\tag{2.22}
$$

Lemma 2.1.4. [45]For any mesh functions $h = \left\{ h^i \mid 0 \leq i \leq N \right\}$ defined on Ω_ζ, the following inequality holds:

$$\Delta\zeta \sum_{i=1}^{n} \left({}_{0}^{FC}\mathbb{D}_{\zeta}^{\gamma} h^i \right) h^i \geq \frac{\zeta_n^{-\gamma} - 2\gamma\varepsilon\zeta_{n-1}}{2\Gamma(1-\gamma)} \Delta\zeta \sum_{i=1}^{n} \left(h^i \right)^2 - \frac{\zeta_n^{1-\gamma} + \gamma(1-\gamma)\varepsilon\zeta_{n-1}\Delta\zeta}{2\Gamma(2-\gamma)} \left(h^0 \right)^2. \quad (2.23)$$

As our fast evaluation approach is used to compute the Caputo fractional derivative, the results in Lemmas 2.1.3 and 2.1.4 can be used to demonstrate the convergence and stability characteristics of the entire numerical scheme for solving time-fractional ODEs.

2.3 Numerical Results and Discussion

This section we apply the fast evalaution of Caputo derivative for solving fractional differential equations here we provide example to assess the accuracy of the method.

Example 1. A linear fractional differential equation of order γ is given as,

$$_{0}^{C}D_{\zeta}^{\gamma}y(\zeta) + \mu(\zeta)\,y(\zeta) = g(\zeta), \quad 0 < \gamma < 1, \quad 2 < \nu < 3, \quad (2.24)$$

with initial condition

$$y(0) = 0,$$

For $\mu(\zeta) = \cos(\zeta) + 0.5\zeta$, $g(\zeta) = (1+\gamma)(\frac{\Gamma(\nu+1.75)}{\Gamma(\nu+1.75-\gamma)}(\zeta)^{(\nu-\gamma+0.75)} + \mu(\zeta)(\zeta)^{(\nu+0.75)})$. The exact solution to this problem is $y(\zeta) = (1+\gamma)(\zeta)^{\nu+0.75}$. By applying the fast evaluation approach with time size 64 on the equation (2.24).

$$\left(\frac{1}{\Gamma(2-\gamma)\Delta\zeta_n{}^\gamma} - \mu(\zeta_n) \right) y(\zeta_n) \approx g(\zeta_n) + \frac{1}{\Gamma(2-\gamma)} \left[\frac{y(\zeta_{n-1})}{(\Delta\zeta_n)^\gamma} \right] - \frac{1}{\Gamma(1-\gamma)} \left[\frac{y(\zeta_{n-1})}{(\Delta\zeta_n)^\gamma} - \frac{y(\zeta_0)}{(\zeta_n)^\gamma} \right]$$

$$-\gamma \sum_{i=1}^{Nexp} w_i \left(e^{-(si\Delta\zeta_n)} y_{hist,i}(\zeta_{n-1}) + \frac{e^{-(si\Delta\zeta_n)}}{si^2\Delta\zeta_{n-1}} \left[(e^{-si\Delta\zeta_{n-1}} - 1 + si\Delta\zeta_{n-1}) y(\zeta_{n-1}) \right. \right.$$

$$\left. \left. + \left(1 - e^{-si\Delta\zeta_{n-1}} - e^{-si\Delta\zeta_{n-1}} si\Delta\zeta_{n-1} \right) y(\zeta_{n-2}) \right] \right). \quad (2.25)$$

The results are illustrated in Figure (2.1), by demonstrating the effectiveness of the approach.
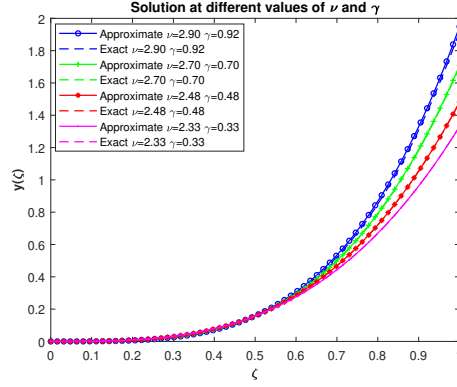
Figure 2.1: The approximate and exact solution at different values of γ and ν.

2.4 Fast Evaluation of Caputo Hadamard Fractional Derivative of Order γ.

In this section, we will consider the fast evaluation technique of the Caputo-Hadamard fractional derivative for $a < \gamma < ae$. Suppose that we would like to evaluate the Caputo-Hadamard fractional derivative on the interval $[a, T]$ over a set of grid points $\Omega_\zeta := \{\zeta_n, n = 0, 1, \cdots, N_T\}$, with $\zeta_0 = 0$, $\zeta_{N_T} = T$, and $\Delta\zeta_n = \zeta_n - \zeta_{n-1}$.

Caputo-Hadamard fractional derivative defined as,

$$
{}^H_\zeta D_a^\gamma y(\zeta)\Big|_{\zeta=\zeta n} = \frac{1}{\Gamma(n-\gamma)} \int_a^{\zeta_n} \left(\log \frac{\zeta_n}{s}\right)^{n-\gamma-1} \delta^n y(s) \frac{ds}{s}. \tag{2.26}
$$

For $a < \gamma < ae$, we have

$$
{}^H_\zeta D_a^\gamma y(\zeta)\Big|_{\zeta=\zeta n} = \frac{1}{\Gamma(1-\gamma)} \int_a^{\zeta_n} \left(\log \frac{\zeta_n}{s}\right)^{-\gamma} \delta y(s) \frac{ds}{s}, \tag{2.27}
$$

we can rewrite the equation (2.27) as follows[44],

$$
{}^H_\zeta D_a^\gamma y(\zeta)\Big|_{\zeta=\zeta n} = \frac{1}{\Gamma(1-\gamma)} \int_a^{\zeta_n} \left(\log \frac{\zeta_n}{a} - \log \frac{s}{a}\right)^{-\gamma} \delta y(s) \frac{ds}{s}, \tag{2.28}
$$

we can see equation (2.28) can be written as $u_n = \log\left(\frac{\zeta_n}{a}\right)$ and $\chi = \log\left(\frac{s}{a}\right)$,

$$
{}^H_\zeta D_a^\gamma y(\zeta)\Big|_{\zeta=\zeta n} = \frac{1}{\Gamma(1-\gamma)} \int_0^{u_n} (u_n - \chi)^{-\gamma} \frac{d\tilde{y}(\chi)}{d\chi} d\chi. \tag{2.29}
$$

Convolution integral separated as following part: history and local part.

$$
\begin{aligned}
{}^H_\zeta D_a^\gamma y(\zeta)\mid_{\zeta=\zeta n} =& \frac{1}{\Gamma(1-\gamma)} \int_0^{u_{n-1}} (u_n - \chi)^{-\gamma} \frac{d\tilde{y}(\chi)}{d\chi} d\chi \\
&+ \frac{1}{\Gamma(1-\gamma)} \int_{u_{n-1}}^{u_n} (u_n - \chi)^{-\gamma} \frac{d\tilde{y}(\chi)}{d\chi} d\chi,
\end{aligned} \tag{2.30}
$$

17

$$\left. {}^{H}_{\zeta} D^{\gamma}_{a} y(\zeta) \right|_{\zeta=\zeta n} := H_n + L_n, \tag{2.31}$$

where

$$H_n\left(u_n\right) = \frac{1}{\Gamma(1-\gamma)} \int_0^{u_{n-1}} \left(u_n - \chi\right)^{-\gamma} \frac{d\tilde{y}(\chi)}{d\chi} d\chi,$$

$$L_n\left(u_n\right) = \frac{1}{\Gamma(1-\gamma)} \int_{u_{n-1}}^{u_n} \left(u_n - \chi\right)^{-\gamma} \frac{d\tilde{y}(\chi)}{d\chi} d\chi,$$

$H_n\left(u_n\right)$ and $L_n\left(u_n\right)$ are history and local part, respectively. For the local part, we approximate $\tilde{y}'(\chi)$ by a constant $\frac{\tilde{y}(u_n) - \tilde{y}\left(u_{n-1}\right)}{\Delta u_n}$ to get,

$$L_n\left(u_n\right) \approx \frac{1}{\Gamma(1-\gamma)} \int_{u_{n-1}}^{u_n} \left(u_n - \chi\right)^{-\gamma} \left[\frac{\tilde{y}\left(u_n\right) - \tilde{y}\left(u_{n-1}\right)}{\Delta u_n}\right] d\chi, \tag{2.32}$$

since

$$L_n\left(u_n\right) \approx \frac{1}{\Gamma(1-\gamma)} \left[\frac{\tilde{y}\left(u_n\right) - \tilde{y}\left(u_{n-1}\right)}{\Delta u_n}\right] \int_{u_{n-1}}^{u_n} \left(u_n - \chi\right)^{-\gamma} d\chi, \tag{2.33}$$

$$L_n\left(u_n\right) \approx \frac{1}{\Gamma(2-\gamma)} \left[\frac{\tilde{y}\left(u_n\right) - \tilde{y}\left(u_{n-1}\right)}{\left(\Delta u_n\right)^{\gamma}}\right]. \tag{2.34}$$

Let $L_n\left(u_n\right) = L_n\left(\log \frac{\zeta_n}{a}\right)$,

$$L_n\left(u_n\right) \approx \frac{1}{\Gamma(2-\gamma)} \left[\frac{y\left(\log \frac{\zeta_n}{a}\right) - y\left(\log \frac{\zeta_{n-1}}{a}\right)}{\left(\log \frac{\zeta_n}{a} - \log \frac{\zeta_{n-1}}{a}\right)^{\gamma}}\right]. \tag{2.35}$$

For the history part,

$$H_n\left(u_n\right) = \frac{1}{\Gamma(1-\gamma)} \int_0^{u_{n-1}} \left(u_n - \chi\right)^{-\gamma} \frac{d\tilde{y}(\chi)}{d\chi} d\chi, \tag{2.36}$$

by applying integration by parts to equation (2.36),

$$H_n\left(u_n\right) = \frac{1}{\Gamma(1-\gamma)} \left[\frac{\tilde{y}\left(u_{n-1}\right)}{\left(\Delta u_n\right)^{\gamma}} - \frac{\tilde{y}\left(u_0\right)}{\left(u_n\right)^{\gamma}} - \gamma \int_0^{u_{n-1}} \frac{\tilde{y}(\chi)}{\left(u_n - \chi\right)^{\gamma}} d\chi\right]. \tag{2.37}$$

To approximate the history part using the Sum-of-Exponential (SOE) approximation for the convolution kernel $u^{-1-\gamma}$, as discussed in section (2.5), we aim to represent the kernel as a sum of exponentials to simplify the computation of convolution integrals.

$$H_n\left(u_n\right) \approx \frac{1}{\Gamma(1-\gamma)} \left[\frac{\tilde{y}\left(u_{n-1}\right)}{\left(\Delta u_n\right)^{\gamma}} - \frac{\tilde{y}\left(u_0\right)}{\left(u_n\right)^{\gamma}} - \gamma \sum_{i=1}^{Nexp} w_i \int_0^{u_{n-1}} e^{-(u_n - \chi)s_i} \tilde{y}(\chi) d\chi\right], \tag{2.38}$$

$$H_n\left(u_n\right) = \frac{1}{\Gamma(1-\gamma)} \left[\frac{\tilde{y}\left(u_{n-1}\right)}{\left(\Delta u_n\right)^{\gamma}} - \frac{\tilde{y}\left(u_0\right)}{\left(u_n\right)^{\gamma}} - \gamma \sum_{i=1}^{Nexp} w_i \tilde{y}_{hist,i}\left(u_n\right)\right], \tag{2.39}$$

18

we introduce a new function $\tilde{y}_{hist,i}(u_n)$ defined as follows:

$$\tilde{y}_{hist,i}(u_n) = \int_0^{u_{n-1}} e^{-(u_n-\chi)s_i}\tilde{y}(\chi)d\chi. \tag{2.40}$$

To evaluate $\tilde{y}_{hist,i}(u_n)$ for $n = 1, 2, \ldots, N_T$, we will observe the following simple recurrence relation:

$$\tilde{y}_{hist,i}(u_n) = \int_0^{u_{n-2}} e^{-(u_n-\chi)s_i}\tilde{y}(\chi)d\chi + \int_{u_{n-2}}^{u_{n-1}} e^{-(u_n-\chi)s_i}\tilde{y}(\chi)d\chi. \tag{2.41}$$

Simplified form of Equation (2.43).

$$\tilde{y}_{hist,i}(u_n) = e^{-(si\Delta u_n)}\tilde{y}_{hist,i}(u_{n-1}) + \int_{u_{n-2}}^{u_{n-1}} e^{-(u_n-\chi)s_i}\tilde{y}(\chi)d\chi, \tag{2.42}$$

where

$$\int_{u_{n-2}}^{u_{n-1}} e^{-(u_n-\chi)s_i}\tilde{y}(\chi)d\chi = \frac{e^{-(si\Delta u_n)}}{si^2\Delta u_{n-1}}\left[\left(e^{-si\Delta u_{n-1}} - 1 + si\Delta u_{n-1}\right)\tilde{y}(u_{n-1}) + \right.$$
$$\left. \left(1 - e^{-si\Delta u_{n-1}} - e^{-si\Delta u_{n-1}}si\Delta u_{n-1}\right)\tilde{y}(u_{n-2})\right]. \tag{2.43}$$

By using equation (2.43) into equation (2.42), we get

$$\tilde{y}_{hist,i}(u_n) = e^{-(si\Delta u_n)}\tilde{y}_{hist,i}(u_{n-1}) + \frac{e^{-(si\Delta u_n)}}{si^2\Delta u_{n-1}}\left[\left(e^{-si\Delta u_{n-1}} - 1 + si\Delta u_{n-1}\right)\tilde{y}(u_{n-1}) + \right.$$
$$\left. \left(1 - e^{-si\Delta u_{n-1}} - e^{-si\Delta u_{n-1}}si\Delta u_{n-1}\right)\tilde{y}(u_{n-2})\right]. \tag{2.44}$$

By applying (2.44) within (2.39) to obtain the history part.

$$H_n(u_n) \approx \frac{1}{\Gamma(1-\gamma)}\left[\frac{\tilde{y}(u_{n-1})}{(\Delta u_n)^\gamma} - \frac{\tilde{y}(u_0)}{(u_n)^\gamma} - \gamma\sum_{i=1}^{Nexp} w_i\left(e^{-(si\Delta u_n)}\tilde{y}_{hist,i}(u_{n-1})\right.\right.$$
$$+ \frac{e^{-(si\Delta u_n)}}{si^2\Delta u_{n-1}}\left[(e^{-si\Delta u_{n-1}} - 1 + si\Delta u_{n-1})\tilde{y}(u_{n-1}) + \left(1 - e^{-si\Delta u_{n-1}}\right.\right.$$
$$\left.\left.\left.\left. -e^{-si\Delta u_{n-1}}si\Delta u_{n-1}\right)\tilde{y}(u_{n-2})\right]\right)\right]. \tag{2.45}$$

Let $H_n\left(u_n\right) = H_n\left(\log \frac{\zeta_n}{a}\right)$,

$$
H_n\left(u_n\right) \approx \frac{1}{\Gamma(1-\gamma)}\left[\frac{y\left(\log \frac{\zeta_{n-1}}{a}\right)}{\left(\log \frac{\zeta_n}{a}-\log \frac{\zeta_{n-1}}{a}\right)^\gamma}-\frac{y\left(\log \frac{\zeta_0}{a}\right)}{\left(\log \frac{\zeta_n}{a}\right)^\gamma}-\gamma \sum_{i=1}^{Nexp} w_i\left(e^{-si\left(\log \frac{t_n}{a}-\log \frac{\zeta_{n-1}}{a}\right)}\right.\right.
$$

$$
y_{hist,i}\left(\log \frac{\zeta_{n-1}}{a}\right)+\frac{e^{-si\left(\log \frac{\zeta_n}{a}-\log \frac{\zeta_{n-1}}{a}\right)}}{si^2\left(\log \frac{\zeta_{n-1}}{a}-\log \frac{\zeta_{n-2}}{a}\right)}\left[\left(e^{-si\left(\log \frac{\zeta_{n-1}}{a}-\log \frac{\zeta_{n-2}}{a}\right)}-1\right.\right.
$$

$$
\left.+si\left(\log \frac{\zeta_{n-1}}{a}-\log \frac{\zeta_{n-2}}{a}\right)\right) y\left(\log \frac{\zeta_{n-1}}{a}\right)+\left(1-e^{-si\left(\log \frac{\zeta_{n-1}}{a}-\log \frac{\zeta_{n-2}}{a}\right)}\right.
$$

$$
\left.\left.\left.\left.-e^{-si\left(\log \frac{\zeta_{n-1}}{a}-\log \frac{t_{n-2}}{a}\right)} si\left(\log \frac{\zeta_{n-1}}{a}-\log \frac{\zeta_{n-2}}{a}\right)\right) y\left(\log \frac{\zeta_{n-2}}{a}\right)\right]\right)\right] . \tag{2.46}
$$

By the combining the equations (2.46) and (2.35), we will get the Fast evaluation technique for the Caputo-Hadamard fractional derivative.

$$
\left.{}^H_\zeta D_a^\gamma y(\zeta)\right|_{\zeta=\zeta_n} \approx \frac{1}{\Gamma(2-\gamma)}\left[\frac{y\left(\log \frac{\zeta_n}{a}\right)-y\left(\log \frac{t_{n-1}}{a}\right)}{\left(\log \frac{\zeta_n}{a}-\log \frac{\zeta_{n-1}}{a}\right)^\gamma}\right]+\frac{1}{\Gamma(1-\gamma)}\left[\frac{y\left(\log \frac{\zeta_{n-1}}{a}\right)}{\left(\log \frac{\zeta_n}{a}-\log \frac{\zeta_{n-1}}{a}\right)^\gamma}\right.
$$

$$
-\frac{y\left(\log \frac{\zeta_0}{a}\right)}{\left(\log \frac{\zeta_n}{a}\right)^\gamma}-\gamma \sum_{i=1}^{Nexp} w_i\left(e^{-si\left(\log \frac{\zeta_n}{a}-\log \frac{\zeta_{n-1}}{a}\right)} y_{hist,i}\left(\log \frac{\zeta_{n-1}}{a}\right)+\right.
$$

$$
\frac{e^{-si\left(\log \frac{\zeta_n}{a}-\log \frac{\zeta_{n-1}}{a}\right)}}{si^2\left(\log \frac{\zeta_{n-1}}{a}-\log \frac{\zeta_{n-2}}{a}\right)}\left[\left(e^{-si\left(\log \frac{\zeta_{n-1}}{a}-\log \frac{\zeta_{n-2}}{a}\right)}-1+si\left(\log \frac{\zeta_{n-1}}{a}\right.\right.\right.
$$

$$
\left.\left.-\log \frac{\zeta_{n-2}}{a}\right)\right) y\left(\log \frac{\zeta_{n-1}}{a}\right)+\left(1-e^{-si\left(\log \frac{\zeta_{n-1}}{a}-\log \frac{\zeta_{n-2}}{a}\right)}-\right.
$$

$$
\left.\left.\left.\left.e^{-si\left(\log \frac{\zeta_{n-1}}{a}-\log \frac{\zeta_{n-2}}{a}\right)} si\left(\log \frac{\zeta_{n-1}}{a}-\log \frac{\zeta_{n-2}}{a}\right)\right) y_{(} \log \frac{\zeta_{n-2}}{a}\right)\right]\right)\right] . \tag{2.47}
$$

2.5 Numerical Results and Discussion

This section deals with solving fractional differential equations using the fast evaluation of Caputo-Hadamard derivative. and provide one numerical example to assess the accuracy of the method.

Example 1. A linear fractional differential equation of order γ is given as,

$$_{\zeta}^{H}D_a^\gamma y\left(\zeta\right) + v_1\left(\zeta\right)y\left(\zeta\right) = g\left(\zeta\right), \quad 0 < \gamma < 1, \quad 0 < \nu < 2, \tag{2.48}$$

with initial condition

$$y(a) = 0,$$

where $v_1\left(\zeta\right) = \sin\left(\zeta\right)$ and $g\left(\zeta\right) = \left(\gamma + 2\nu\right)\left(\frac{\Gamma(\nu+2)}{\Gamma(\nu+2-\gamma)}\left(\log\frac{\varsigma}{a}\right)^{(\nu-\gamma+1)} + v_1\left(\zeta\right)\left(\log\frac{\varsigma}{a}\right)^{(\nu+1)}\right)$. The exact solution of the equation is $y\left(\zeta\right) = \left(\gamma + 2\nu\right)\left(\left(\log\frac{\varsigma}{a}\right)^{\nu+1}\right)$. By applying the current technique with time size 64 on the equation (2.48), the results are illustrated in Figure (2.2), by demonstrating the effectiveness of the approach.
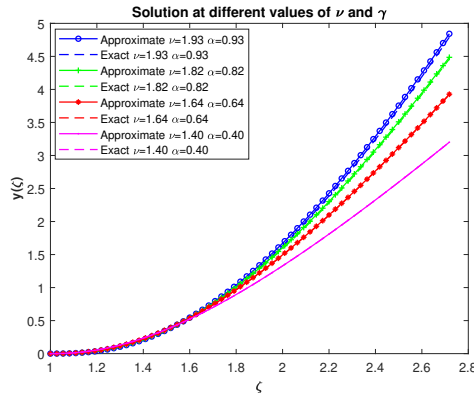
Figure 2.2: The numerical and exact solution at different values of γ and ν.

2.6 Conclusion

The Caputo and Caputo-Hadamard fractional differential equations were effectively solved using fast evaluation techniques. The accuracy plots in Figures 2.1 and 2.2, comparing exact and numerical solutions, demonstrated that our method maintains considerable reliability with the exact solutions. From the results, it is shown that our technique is reliable for solution of fractional differential equations.

Chapter 3

Hadamard Gegenbauer Wavelets Method

Gegenbauer wavelets, derived from Gegenbauer polynomials, are effective method for solving fractional differential equations (FDEs) due to their orthogonality and strong approximation capabilities. Bhrawy et al. [54] demonstrated the effectiveness of Gegenbauer wavelets in solving multi-term FDEs, showing their accuracy in discretizing fractional derivatives. The Hadamard fractional derivative, which includes a logarithmic kernel, creates specific challenges in solving initial value problems. However, Gegenbauer wavelets have proven effective in addressing these problems. Doha et al. showed how to use Gegenbauer wavelets for Hadamard derivatives, improving the precision of solutions to initial value problems. Additionally, Aboodh et al. [58] combined Gegenbauer wavelets with the Galerkin method to solve nonlinear differential equations, resulting in better accuracy and stability. Applications of Gegenbauer wavelets in solving Hadamard fractional differential equations in various fields. For instance, El-Gamel et al. [57] used them for electromagnetic wave propagation, and Zhu et al. [56] applied them to fluid dynamics problems, demonstrating their efficiency and effectiveness in practical scenarios.

3.1 Gegenbauer Polynomails

The Gegenbauer polynomails also known as ultraspherical harmonics polynomails C_n^ρ, with order n, are defined for $\rho > -1/2$ and $n \in Z^+$, with in the interval $[0, 1]$.

$$C_n^\rho(x) = \frac{\Gamma(\rho + 0.5)}{\Gamma(2\rho)} \sum_{i=0}^{n} \frac{(-1)^{i+n}\Gamma(2\rho + i + n)}{(i)!(n-i)!\Gamma(i + \rho + 0.5)}(x)^i. \tag{3.1}$$

To utilize these polynomails over the interval [0,1], introduce the Fractional Gegenbauer polynomials. By transformation, where the new variable s is introduced as $x = s^\gamma$,

$$C_n^{\rho,\gamma}(s) = \frac{\Gamma(\rho + 0.5)}{\Gamma(2\rho)} \sum_{i=0}^{n} \frac{(-1)^{i+n}\Gamma(2\rho + i + n)}{(i)!(n-i)!\Gamma(i + \rho + 0.5)}(s)^{i\gamma}. \tag{3.2}$$

3.1.1 Hadamard Gegenbauer Wavelets

We have developed new wavelets, by using the transformation from Gegenbauer polynomials, modifying the interval from $[0, 1)$ to $[a, ae)$. These newly developed wavelets are referred to as Hadamard

Gegenbauer wavelets (HGW).

$$\Phi_{m,n}^{\rho,\gamma}(\zeta) = \begin{cases} 2^{\frac{k}{2}} C_n^{\rho,\alpha}\left(2^k \log \frac{\zeta}{ae^{\frac{m}{2^k}}}\right)^{i\gamma}, & ae^{\frac{m}{2^k}} < \zeta \le ae^{\frac{m+1}{2^k}}, \\ 0, & \text{elsewhere}, \end{cases} \tag{3.3}$$

where $k = 0, 1, 2, \ldots$, is the level of resolution and $m = 0, 1, 2, \ldots, 2^k - 1$, is the translation parameter, while $n = 0, 1, 2, \ldots, N - 1, N^+$ is the order of Gegenbauer polynomials and $\rho > -1/2$.

3.2 Function Approximations and the Hadamard Gegenbauer Matrix.

A function $y(\zeta) \in \mathrm{L}^p[a, ae)$ can be represented by a truncated series of HGW.

$$y(\zeta) \approx \sum_{m=0}^{2^k-1} \sum_{n=0}^{N-1} c_{m,n}^{\rho} \Phi_{m,n}^{\rho,\gamma}(\zeta) = \mathcal{C}^{\rho} \Phi^{\rho,\gamma}(\zeta), \tag{3.4}$$

where matrices $\mathcal{C}^{\rho}$ and $\Phi^{\rho,\gamma}(\zeta)$ have order of $\hat{p} \times 1$, and $1 \times \hat{p}$, $\hat{p} = 2^k(M+1)$, as follows,

$$\mathcal{C}^{\rho} = \left[c_{10}^{\rho}, c_{11}^{\rho}, \cdots, c_{1N-1}^{\rho}, c_{20}^{\rho}, c_{21}^{\rho}, \cdots, c_{2N-1}^{\rho}, \cdots, c_{2^{k-1}0}^{\rho}, c_{2^{k-1}1}^{\rho}, \cdots, c_{2^{k-1}N-1}^{\rho} \right],$$

$$\Phi^{\rho,\gamma}(\zeta) = \left[\Phi_{0,0}^{\rho,\gamma}(\zeta), \Phi_{0,1}^{\rho,\gamma}(\zeta), \cdots, \Phi_{1,N-1}^{\rho,\gamma}(\zeta), \Phi_{1,0}^{\rho,\gamma}(\zeta), \Phi_{1,1}^{\rho,\gamma}(\zeta), \cdots, \Phi_{1,N-1}^{\rho,\gamma}(\zeta), \cdots \right.$$

$$\left. \Phi_{2^{k-1},0}^{\rho,\gamma}(\zeta), \Phi_{2^{k-1},1}^{\rho,\gamma}(\zeta), \cdots, \Phi_{2^{k-1},N-1}^{\rho,\rho}(\zeta) \right]^t,$$

$\zeta_i = ae^{\frac{2i-1}{2\hat{p}}}$, $\quad i = 1, 2, \ldots \hat{p}$, are collocation points for HGW. The HGW matrix $\Phi_{\hat{p},\hat{p}}^{\rho,\gamma}$ is given by,

$$\Phi_{\hat{p}\times\hat{p}}^{\rho,\gamma} = \left[\Phi^{\rho,\gamma}\left(ae^{\frac{1}{2\hat{p}}}\right), \Phi^{\rho,\gamma}\left(ae^{\frac{3}{2\hat{p}}}\right), \ldots, \Phi^{\rho,\gamma}\left(ae^{\frac{2\hat{p}-1}{2\hat{p}}}\right) \right]. \tag{3.5}$$

or

$$\Phi_{\hat{p}\times\hat{p}}^{\rho,\gamma} = \begin{bmatrix} \Phi_{1,0}^{\rho;\gamma}\left(ae^{\frac{1}{2\hat{p}}}\right) & \Phi_{1,0}^{\rho;\gamma}\left(ae^{\frac{3}{2\hat{p}}}\right) & \cdots & \Phi_{1,0}^{\rho;\gamma}\left(ae^{\frac{2\hat{p}-1}{2\hat{p}}}\right) \\ \Phi_{1,1}^{\rho;\gamma}\left(ae^{\frac{1}{2\hat{p}}}\right) & \Phi_{1,1}^{\rho;\gamma}\left(ae^{\frac{3}{2\hat{p}}}\right) & \cdots & \Phi_{1,1}^{\rho;\gamma}\left(ae^{\frac{2\hat{p}-1}{2\hat{p}}}\right) \\ \vdots & \vdots & \cdots & \vdots \\ \Phi_{1,N-1}^{\rho;\gamma}\left(ae^{\frac{1}{2\hat{p}}}\right) & \Phi_{1,N-1}^{\rho;\gamma}\left(ae^{\frac{3}{2\hat{p}}}\right) & \cdots & \Phi_{1,N-1}^{\rho;\gamma}\left(ae^{\frac{2\hat{p}-1}{2\hat{p}}}\right) \\ \Phi_{2,0}^{\rho;\gamma}\left(ae^{\frac{1}{2\hat{p}}}\right) & \Phi_{2,0}^{\rho;\gamma}\left(ae^{\frac{3}{2\hat{p}}}\right) & \cdots & \Phi_{2,0}^{\rho;\gamma}\left(ae^{\frac{2\hat{p}-1}{2\hat{p}}}\right) \\ \Phi_{2,1}^{\rho;\gamma}\left(ae^{\frac{1}{2\hat{p}}}\right) & \Phi_{2,1}^{\rho;\gamma}\left(ae^{\frac{3}{2\hat{p}}}\right) & \cdots & \Phi_{2,1}^{\rho;\gamma}\left(ae^{\frac{2\hat{p}-1}{2\hat{p}}}\right) \\ \vdots & \vdots & \cdots & \vdots \\ \Phi_{2,N-1}^{\rho;\gamma}\left(ae^{\frac{1}{2\hat{p}}}\right) & \Phi_{2,N-1}^{\rho;\gamma}\left(ae^{\frac{3}{2\hat{p}}}\right) & \cdots & \Phi_{2,N-1}^{\rho;\gamma}\left(ae^{\frac{2\hat{p}-1}{2\hat{p}}}\right) \\ \vdots & \vdots & \cdots & \vdots \\ \Phi_{2^k-1,0}^{\rho;\gamma}\left(ae^{\frac{1}{2\hat{p}}}\right) & \Phi_{2^k-1,0}^{\rho;\gamma}\left(ae^{\frac{3}{2\hat{p}}}\right) & \cdots & \Phi_{2_1^k,0}^{\rho;\gamma}\left(ae^{\frac{2\hat{p}-1}{2\hat{p}}}\right) \\ \Phi_{2^k-1,1}^{\rho;\gamma}\left(ae^{\frac{1}{2\hat{p}}}\right) & \Phi_{2^k-1,1}^{\rho;\gamma}\left(ae^{\frac{3}{2\hat{p}}}\right) & \cdots & \Phi_{2_1^k,1}^{\rho;\gamma}\left(ae^{\frac{2\hat{p}-1}{2\hat{p}}}\right) \\ \vdots & \vdots & \cdots & \vdots \\ \Phi_{2^k-1,N-1}^{\rho;\gamma}\left(ae^{\frac{1}{2\hat{p}}}\right) & \Phi_{2^k-1,N-1}^{\rho;\gamma}\left(ae^{\frac{3}{2\hat{p}}}\right) & \cdots & \Phi_{2_1^k,N-1}^{\rho;\gamma}\left(ae^{\frac{2\hat{p}-1}{2\hat{p}}}\right) \end{bmatrix}.$$

By fixing the values of the parameters $a = 1 > 0$, $\gamma = 0.5$, $M = 1$, and $k = 2$, we attain $m = 0, 1$, $n = 0, 1, 2, 3$, and $i = 1, 2, \ldots, 8$. Then, the HGW matrix for ρ is given as:

$$\Phi_{8\times 8}^{1.567,m,n} = \begin{bmatrix} 2.0 & 2.0 & 0 & 0 & 0 & 0 & 0 & 0 \\ 0 & 0 & 2.0 & 2.0 & 0 & 0 & 0 & 0 \\ 0 & 0 & 0 & 0 & 2.0 & 2.0 & 0 & 0 \\ 0 & 0 & 0 & 0 & 0 & 0 & 2.0 & 2.0 \\ 0 & 4.5885 & 0 & 0 & 0 & 0 & 0 & 0 \\ 0 & 0 & 0 & 4.5885 & 0 & 0 & 0 & 0 \\ 0 & 0 & 0 & 0 & 0 & 4.5885 & 0 & 0 \\ 0 & 0 & 0 & 0 & 0 & 0 & 0 & 4.5885 \end{bmatrix}.$$

Similarly, various HGW can be obtained by choosing different values for ρ and γ.

3.3   The HGW Operational Matrix of Fractional order Integral

Apply HGW fractional order integral operator of order η over HGW as:

$$_\zeta I_a^\eta \Phi_{m,n}(\zeta) = 2^{\frac{k}{2}} {}_\zeta I_a^\eta C_n^{\rho,\gamma} \left(2^k \log \frac{\zeta}{ae^{\frac{m}{2^k}}}\right)^{i\gamma}. \tag{3.7}$$

By using the equation (3.2), we get.

$$\zeta I_a^\eta \Phi_{m,n}(\zeta) = 2^{k(0.5+i\gamma)} \frac{\Gamma(\rho+0.5)}{\Gamma(2\rho)} \sum_{i=0}^{n} \frac{(-1)^{i+n}\Gamma(2\rho+i+n)}{(i)!(n-i)!\Gamma(i+\rho+0.5)} \zeta I_a^\eta \left(\log \frac{\zeta}{ae^{\frac{m}{2^k}}} \right)^{i\gamma}. \quad (3.8)$$

After applying the Caputo-Hadamard fractional integral, we obtain.

$$\zeta I_a^\eta \Phi_{m,n}(\zeta) = 2^{k(0.5+i\gamma)} \frac{\Gamma(\rho+0.5)}{\Gamma(2\rho)} \sum_{i=0}^{n} \frac{(-1)^{i+n}\Gamma(2\rho+i+n)}{(i)!(n-i)!\Gamma(i+\rho+0.5)} \frac{\Gamma(i\gamma+1)}{\Gamma(i\gamma+\eta+1)} \left(\log \frac{\zeta}{ae^{\frac{m}{2^k}}} \right)^{i\gamma+\eta}. \quad (3.9)$$

For $\zeta \geq ae^{\frac{m+1}{2^k}}$,

$$\zeta I_{a,ae}^\eta \Phi_{m,n}(\zeta) = 2^{k(0.5+i\gamma)} \frac{\Gamma(\rho+0.5)}{\Gamma(2\rho)} \sum_{i=0}^{n} \frac{(-1)^{i+n}\Gamma(2\rho+i+n)}{(i)!(n-i)!\Gamma(i+\rho+0.5)} \zeta I_{a,ae}^\eta \left(\log \frac{\zeta}{ae^{\frac{m}{2^k}}} \right)^{i\gamma}, \quad (3.10)$$

$$= 2^{k(0.5+i\gamma)} \frac{\Gamma(\rho+0.5)}{\Gamma(2\rho)\Gamma(\eta)} \sum_{i=0}^{n} \frac{(-1)^{i+n}\Gamma(2\rho+i+n)}{(i)!(n-i)!\Gamma(i+\rho+0.5)} \int_{ae^{\frac{m}{2^k}}}^{ae^{\frac{m+1}{2^k}}} \frac{1}{\tau} \left(\log \left(\frac{\zeta}{\tau} \right) \right)^{\eta-1} \left(\log \left(\frac{\tau}{ae^{\frac{n}{2^k}}} \right) \right)^{i\gamma} d\tau, \quad (3.11)$$

$$= 2^{k(0.5+i\gamma)} \frac{\Gamma(\rho+0.5)}{\Gamma(2\rho)\Gamma(\eta)} \sum_{i=0}^{n} \frac{(-1)^{i+n}\Gamma(2\rho+i+n)}{(i)!(n-i)!\Gamma(i+\rho+0.5)} w(\zeta), \quad (3.12)$$

where $w(\zeta) = \int_{ae^{\frac{m}{2^k}}}^{ae^{\frac{m+1}{2^k}}} \frac{1}{\tau} \left(\log \left(\frac{\zeta}{\tau} \right) \right)^{\eta-1} \left(\log \left(\frac{\tau}{ae^{\frac{m}{2^k}}} \right) \right)^{i\gamma} ds$, It can be assessed using the global adaptive technique with different parameter values of m and n in MATLAB R2024a. Generally, we have the following expression for the η-order Caputo-Hadamard fractional integral of HGW.

$$\zeta I_a^\eta \Phi_{m,n}(\zeta) = 2^{k(0.5+i\gamma)} \frac{\Gamma(\rho+0.5)}{\Gamma(2\rho)} \sum_{i=0}^{n} \frac{(-1)^{i+n}\Gamma(2\rho+i+n)}{(i)!(n-i)!\Gamma(i+\rho+0.5)}$$

$$\begin{cases} \frac{\Gamma(i\gamma+1)}{\Gamma(i\gamma+\eta+1)} \left(\log \frac{\zeta}{ae^{\frac{m}{2^k}}} \right)^{i\gamma+\eta}, & ae^{\frac{m}{2^k}} \leq \zeta < ae^{\frac{m+1}{2^k}}, \\ \frac{1}{\Gamma(\eta)} w(\zeta), & \zeta \geq ae^{\frac{m+1}{2^k}}. \end{cases} \quad (3.13)$$

Let $B_{m,n}^\eta(\zeta) = \zeta I_a^\eta \Phi_{m,n}(\zeta)$. We can represent. (3.13) in vector form as,

$$\mathbf{B}_{m,n}^\eta(\zeta) = \Big[B_{0,0}^\eta(\zeta), B_{0,1}^\eta(\zeta), \cdots, B_{0,R-1}^\eta(\zeta), B_{1,0}^\eta(\zeta), B_{1,1}^\eta(\zeta), \cdots, B_{1,N-1}^\eta(\zeta),$$

$$\cdots, B_{2^k-1,0}^\eta(\zeta), B_{2^k-1,1}^\eta(\zeta), \cdots, B_{2^k-1,N-1}^\eta(\zeta) \Big]^T. \quad (3.14)$$

Evaluate (3.14) at the collocation points $\zeta_i = ae^{\frac{2i-1}{2\hat{p}}}$, $i = 1, 2, \ldots, \hat{p}$, we get,

$$\mathbf{B}_{\hat{p}\times\hat{p}}^{\eta,m,n} = \left[\mathbf{B}_{m,n}^\eta \left(ae^{\frac{1}{2\hat{p}}} \right), \mathbf{B}_{m,n}^\eta \left(ae^{\frac{3}{2\hat{p}}} \right), \cdots, \mathbf{B}_{m,n}^\eta \left(ae^{\frac{2\hat{p}-1}{2\hat{p}}} \right) \right]. \quad (3.15)$$

25

In particular, for the parameters $a = 1 > 0$, $k = 2$, $M = 1$, $\rho = 1$, and $\eta = 1.5$, with $n = 0, 1, 2, 3$ and $m = 0, 1, 2$, the Caputo-Hadamard fractional integration matrix of order η for the HGW is given as follows.

$$\mathbf{B}_{8\times 8}^{1.5,m,n} = \begin{bmatrix} 0.0235 & 0.1222 & 0.2393 & 0.3132 & 0.3719 & 0.4223 & 0.4672 & 0.5080 \\ 0 & 0 & 0.0235 & 0.1222 & 0.2393 & 0.3132 & 0.3719 & 0.4223 \\ 0 & 0 & 0 & 0 & 0.0235 & 0.1222 & 0.2393 & 0.3132 \\ 0 & 0 & 0 & 0 & 0 & 0 & 0.0235 & 0.1222 \\ -0.0376 & -0.0977 & -0.0564 & -0.0426 & -0.0358 & -0.0315 & -0.0284 & -0.0261 \\ 0 & 0 & -0.0376 & -0.0977 & -0.0564 & -0.0426 & -0.0358 & -0.0315 \\ 0 & 0 & 0 & 0 & -0.0376 & -0.0977 & -0.0564 & -0.0426 \\ 0 & 0 & 0 & 0 & 0 & 0 & -0.0376 & -0.0977 \end{bmatrix}.$$

3.4 The HGW Operational Matrix of Caputo-Hadamard fractional integration for BVP

It is important to apply an additional operational matrix of Caputo-Hadamard fractional integration to control the boundary conditions in order to solve the Caputo-Hadamard fractional boundary value problem. Using the η Caputo-Hadamard fractional integral from a to ae on $\Phi_{m,n}(\zeta)$, we achieve the following:

$$_{\zeta}I_a^{\eta}\Phi_{m,n}^{\rho,\gamma}(\zeta) = \frac{1}{\Gamma(\eta)} \int_a^{\zeta} (\frac{1}{\tau}) \log(\frac{\zeta}{\tau})^{\eta-1} \Phi_{m,n}^{\rho,\gamma}(\tau) d\tau, \tag{3.16}$$

$$_{\zeta}I_a^{\eta}\Phi_{m,n}^{\rho,\gamma}(e) = \frac{1}{\Gamma(\eta)} \int_{ae^{\frac{m}{2^k}}}^{ae^{\frac{m+1}{2^k}}} (\frac{1}{\tau}) \log(\frac{e}{\tau})^{\eta-1} \Phi_{m,n}^{\rho,\gamma}(\tau) d\tau, \tag{3.17}$$

$$= \frac{1}{\Gamma(\eta)} 2^{k(0.5+i\gamma)} \frac{\Gamma(\rho+0.5)}{\Gamma(2\rho)} \sum_{i=0}^{n} \frac{(-1)^{i+n}\Gamma(2\rho+i+n)}{(i)!(n-i)!\Gamma(i+\rho+0.5)} \int_{ae^{\frac{m}{2^k}}}^{ae^{\frac{m+1}{2^k}}} (\frac{1}{\tau}) \log(\frac{e}{\tau})^{\eta-1} \log(\frac{\tau}{a})^{i\gamma} d\tau, \tag{3.18}$$

$$= \frac{1}{\Gamma(\eta)} 2^{k(0.5+i\gamma)} \frac{\Gamma(\rho+0.5)}{\Gamma(2\rho)} \sum_{i=0}^{n} \frac{(-1)^{i+n}\Gamma(2\rho+i+n)}{(i)!(n-i)!\Gamma(i+\rho+0.5)} u^{\eta,k,m,n}, \tag{3.19}$$

where $u^{\eta,k,m,n} = \int_{ae^{\frac{m}{2^k}}}^{ae^{\frac{m+1}{2^k}}} \left(\frac{1}{\tau}\right) \log\left(\frac{e}{\tau}\right)^{\eta-1} \log\left(\frac{\tau}{a}\right)^{i\gamma} d\tau$, for $m = 0, 1, 2, \ldots, 2^k-1$, and $n = 0, 1, 2, \ldots, N-1$, with $N \in \mathbb{Z}^+$. The vector form of $u^{\gamma,k,m,n}$ is given as follows:

$$U_{\hat{p}\times 1}^{\eta,k,m,n} = [u^{\eta,k,0,0}, u^{\eta,k,0,1}, \cdots, u^{\eta,k,0,N}, u^{\eta,k,1,0}, u^{\eta,k,1,1}, \cdots, u^{\eta,k,1,N}, \cdots, u^{\eta,k,2^p-1,0}, u^{\eta,k,2^p-1,1}$$
$$, \cdots, u^{\eta,k,2^p-1,N}]^T. \tag{3.20}$$

We can evaluate the components of $U_{\hat{p}\times 1}^{\eta,m,n}$ using the global adaptive technique in MATLAB R2024a. Given the parameters $a = 1$, $k = 2$, $\gamma = 0.68$, $p = 2$, $M = 1$, and $\rho = 1.465$, with the integral order

defined as $\eta = 1.789$, we obtain the following:

$$U_{8\times 1}^{1.789,m,n} = [0.4844, 0.3712, 0.2476, 0.1008, -0.0534, -0.0573, -0.0640, -0.0837]^T.$$

Consider any function $d(\zeta) \in L^2[0,1]$, we have

$$d(\zeta)I_a^\eta \Phi_{m,n}^{\rho,\gamma}(e) = d(\zeta)\frac{1}{\Gamma(\beta)} 2^{k(0.5+i\gamma)} \frac{\Gamma(\rho+0.5)}{\Gamma(2\rho)} \sum_{i=0}^{n} \frac{(-1)^{i+n}\Gamma(2\rho+i+n)}{(i)!(n-i)!\Gamma(i+\rho+0.5)} u^{\eta,k,m,n}. \qquad (3.21)$$

Expand (3.21) at the collocation points to get.

$$\mathbf{Q}_{\hat{p}\times\hat{p}}^{b(\zeta),\eta,m,n} = U_{\hat{p}\times 1}^{\eta,m,n} \mathbf{D}_{1\times\hat{p}},$$

where $\mathbf{D}_{1\times\hat{p}} = \left[d(\zeta_1), d(\zeta_2), \cdots, d(\zeta_{\hat{p}}) \right]$. For $d(\zeta) = \sin(\zeta), \rho = 2, M = 1$, k=2 and $\gamma = 0.787$, The order of integral is defined as $\eta = 1.768$, we obtain.

$$\mathbf{Q}_{8\times 8}^{1.768,m,n} = \begin{bmatrix} 0.4272 & 0.4564 & 0.4783 & 0.4883 & 0.4802 & 0.4464 & 0.3790 & 0.2710 \\ 0.3297 & 0.3522 & 0.3692 & 0.3769 & 0.3706 & 0.3446 & 0.2925 & 0.2091 \\ 0.2222 & 0.2374 & 0.2489 & 0.2541 & 0.2498 & 0.2322 & 0.1972 & 0.1410 \\ 0.0924 & 0.0987 & 0.1034 & 0.1056 & 0.1038 & 0.0965 & 0.0819 & 0.0586 \\ -0.0626 & -0.0668 & -0.0701 & -0.0715 & -0.0703 & -0.0654 & -0.0555 & -0.0397 \\ -0.0677 & -0.0723 & -0.0758 & -0.0774 & -0.0761 & -0.0707 & -0.0600 & -0.0429 \\ -0.0764 & -0.0816 & -0.0855 & -0.0873 & -0.0858 & -0.0798 & -0.0677 & -0.0484 \\ -0.1027 & -0.1097 & -0.1150 & -0.1174 & -0.1154 & -0.1073 & -0.0911 & -0.0651 \end{bmatrix}.$$

3.5 Error analysis

In this section, we will conduct an error analysis of the Hadamard Gegenbauer wavelet method.

Theorem 3.1.1.[47] Assume that n, k approaches to ∞, then $\sum_{m=0}^{2^k-1} \sum_{n=0}^{N-1} C_{m,n}^\rho \Phi_{m,n}^{\rho,\gamma}(\zeta)$ given in (3.4), converges to $G(\zeta)$. Proof. Consider the inner product of $\Phi_{m,n}^{\rho,\gamma}(\zeta)$ and $G(\zeta)$, we have

$$f_{m,n} = \left\langle G(\zeta), \Phi_{m,n}^{\rho,\gamma}(\zeta) \right\rangle_{\psi H^2(J)} = \int_J G(\zeta)\eta_{m,n}^{\rho,\gamma}(\zeta)g'(\zeta)d\zeta, \qquad (3.22)$$

let we define,

$$S_{k,N} = \sum_{m=1}^{r} \sum_{n=0}^{s} C_{m,n}^\rho \Phi_{m,n}^{\rho,\gamma}(\zeta),$$

where $r = 2^k - 1$ and $s = N - 1$. Firstly, we prove that $S_{k,N}$ is a Cauchy sequence in the Hilbert space $\psi H^2(J)$, $J = [0,1]$. Then, we show that when k and N approach ∞, $S_{k,N}$ converges to $G(\zeta)$. Let

$$B = \{0, 1, 2, \cdots, s^*, s^* + 1, \cdots, s - 1, s\},$$

and

$$S_{k^*,N^*} = \sum_{m=1}^{r^*} \sum_{n=0}^{s^*} C_{mn}^\rho \Phi_{m,n}^{\rho,\gamma}(\zeta),$$

with $r > r^*$ and $s > s^*$.

$$\left\| S_{k,N} - S_{k^*,N^*} \right\|^2 = \left\| \sum_{m=r^*+1}^{r} \sum_{n\in B} C_{m,n}^{\rho} \Phi_{m,n}^{\rho,\gamma}(\zeta) \right\|^2,$$

$$= \sum_{m=r^*+1}^{r} \sum_{n\in B} \sum_{m^*=r^*+1}^{r} \sum_{n^*\in B} C_{mn}^{\rho} C_{m^*n^*}^{\rho} \int_J \Phi_{m,n}^{\rho,\gamma}(\zeta) \eta_{m^*,n^*}^{\rho,\gamma}(\zeta)(g)'(\zeta) d\zeta,$$

$$= \sum_{m=r^*+1}^{r} \sum_{n\in B} \left| C_{m,n}^{\rho} \right|^2. \tag{3.23}$$

By Bessel's inequality, $\sum_{m=r^*+1}^{r} \sum_{n\in B} \left| C_{m,n}^{\rho} \right|^2$ is convergent, and $\left\| S_{k,M} - S_{k^*,M^*} \right\|^2 \to 0$ as $k, N, k^*, N^* \to \infty$,

The sequence $S_{k,N}$ is given by:

$$S_{k,N} = \sum_{m=1}^{r} \sum_{n=0}^{s} C_{mn}^{\rho} \Phi_{m,n}^{\rho,\gamma}(\zeta),$$

We claim that this sequence $\{S_{k,N}\}$ is a Cauchy sequence in $H^2(J)$, and it converges to some function $l(\zeta) \in H^2(J)$. Formally, we write:

$$\lim_{k,N\to\infty} \sum_{m=1}^{r} \sum_{n=0}^{s} C_{mn}^{\rho} \Phi_{m,n}^{\rho,\gamma}(\zeta) = l(\zeta),$$

We show that $l(\zeta) = G(\zeta)$.

Let

$$\left\langle l(\zeta) - G(\zeta), \Phi_{m,n}^{\rho,\gamma}(\zeta) \right\rangle = \left\langle l(\zeta), \Phi_{m,n}^{\rho,\gamma}(\zeta) \right\rangle - \left\langle G(\zeta), \Phi_{m,n}^{\Phi,\gamma}(\zeta) \right\rangle,$$

$$= \lim_{m,n\to\infty} \left\langle S_{k,N}, \Phi_{m,n}^{\rho,\gamma}(\zeta) \right\rangle - f_{n,m}, \tag{3.24}$$

$$= 0.$$

3.6 Initial Value Problems

The suggested approach is implemented for Caputo-Hadamard fractional initial value problems (IVPs).

Consider the general form of linear Caputo-Hadamard fractional IVP DE from the following,

$$_{\zeta}^{H} D_a^{\eta} y(\zeta) + v_1(\zeta)_{\zeta}^{H} D_a^{\gamma} y(\zeta) + v_2(\zeta)_{\zeta}^{H} D_a y(\zeta) + v_3(\zeta) y(\zeta) = h(\zeta),$$

$$a < \zeta \leq ae, \quad 1 < \eta \leq 2, \quad 0 < \gamma \leq 1, \tag{3.25}$$

$$y(a) = s_1, \quad _{\zeta}^{H} D_a y(a) = s_2.$$

Applying the Gegenbauer wavelet series to approximate the higher order term, as explained in (3.4).

$$_{\zeta}^{H} D_a^{\eta} y(\zeta) = \sum_{m=0}^{2^k-1} \sum_{n=0}^{N-1} c_{m,n}^{\rho} \Phi_{m,n}^{\rho,\gamma}(\zeta). \tag{3.26}$$

28

Take fractional integration of (3.26) and after utilizing the Gegenbauer wavelets, we have

$$y(\zeta) = \sum_{m=0}^{2^k-1} \sum_{n=0}^{N-1} c_{m,n}^\rho \zeta I_a^\eta \Phi_{m,n}^{\rho,\gamma}(\zeta) + s_2(\ln(\zeta) - \ln(a)) + s_1, \qquad (3.27)$$

Differentiate equation (3.27), we obtain

$$_\zeta^H D_a y(\zeta) = \sum_{m=0}^{2^k-1} \sum_{n=0}^{N-1} c_{m,n}^\rho \zeta I_a^{\eta-1} \Phi_{m,n}^{\rho,\gamma}(\zeta) + \Gamma(2)s_2, \qquad (3.28)$$

and

$$_\zeta^H D_a^\gamma y(\zeta) = \sum_{m=0}^{2^k-1} \sum_{n=0}^{N-1} c_{m,n}^\rho \zeta I_a^{\eta-\gamma} \Phi_{m,n}^{\rho,\gamma}(\zeta) + \frac{s_2\Gamma(2)}{\Gamma(2-\gamma)}(\ln(\zeta))^{1-\gamma}. \qquad (3.29)$$

Substitute the values of $_\zeta^H D_a^\eta y(\zeta), y(\zeta), _\zeta^H D_a^1 y(\zeta)$, and $_\zeta^H D_a^\gamma y(\zeta)$ from equations (3.26), (3.27), (3.28) and (3.29) in (3.25), we get

$$\sum_{m=0}^{2^k-1} \sum_{n=0}^{N-1} c_{m,n}^\rho \left[\Phi_{m,n}^{\rho,\gamma}(\zeta) + \zeta I_a^{\eta-\gamma}(\zeta)\Phi_{m,n}^{\rho,\gamma}(\zeta)v_1(\zeta) + \zeta I_a^{\eta-1}(\zeta)\Phi_{m,n}^{\rho,\gamma}(\zeta)v_2(\zeta) + \zeta I_a^\eta(\zeta)\Phi_{m,n}^{\rho,\gamma}(\zeta)v_3(\zeta) \right] = h(\zeta)$$

$$- \frac{s_2\Gamma(2)}{\Gamma(2-\gamma)}(\ln(\zeta))^{1-\gamma}v_1(\zeta) - \Gamma(2)s_2 v_2(\zeta) - \left(s_2(\ln(\zeta) - \ln(a)) + s_1 \right) v_3(\zeta), \qquad (3.30)$$

where

$$F(\zeta) = h(\zeta) - \frac{s_2\Gamma(2)}{\Gamma(2-\gamma)}(\ln(\zeta))^{1-\gamma}v_1(\zeta) - \Gamma(2)s_2 v_2(\zeta) - \left(s_2(\ln(\zeta) - \ln(a)) + s_1 \right) v_3(\zeta),$$

In vector notation, the above equation at collocation points, $\zeta_i = \frac{2i-1}{2\hat{p}}$, where $l = 1, 2, \ldots, \hat{\rho}$, takes the following form,

$$\boldsymbol{C}^\rho \left[\boldsymbol{\Phi}_{\hat{p},\hat{p}}^{\rho,\gamma}(\zeta) + \boldsymbol{B}_{\hat{p},\hat{p}}^{\eta-\gamma}(\zeta)v_1(\zeta) + \boldsymbol{B}_{\hat{p},\hat{p}}^{\eta-1}(\zeta)v_2(\zeta) + \boldsymbol{B}_{\hat{p},\hat{p}}^\eta(\zeta)v_3(\zeta) \right] = \boldsymbol{F_{1\times\hat{p}}}(\zeta), \qquad (3.31)$$

$\mathcal{F}_{1\times\hat{p}} = \left[F(\zeta_1), F(\zeta_2), \ldots, F(\zeta_{\hat{p}}) \right]$, and the diagonal matrices $\boldsymbol{v_1}, \boldsymbol{v_2}$ & $\boldsymbol{v_3}$ are given as

$$\boldsymbol{v_1} = \begin{bmatrix} v_1(\zeta_1) & 0 & \cdots & 0 \\ 0 & v_1(\zeta_2) & \cdots & 0 \\ \vdots & \vdots & \ddots & \vdots \\ 0 & 0 & \cdots & v_1(\zeta_{\hat{p}}) \end{bmatrix}, \boldsymbol{v_2} = \begin{bmatrix} v_2(\zeta_1) & 0 & \cdots & 0 \\ 0 & v_2(\zeta_2) & \cdots & 0 \\ \vdots & \vdots & \ddots & \vdots \\ 0 & 0 & \cdots & v_2(\zeta_{\hat{p}}) \end{bmatrix}$$

and

$$\boldsymbol{v_3} = \begin{bmatrix} v_3(\zeta_1) & 0 & \cdots & 0 \\ 0 & v_3(\zeta_2) & \cdots & 0 \\ \vdots & \vdots & \ddots & \vdots \\ 0 & 0 & \cdots & v_3(\zeta_{\hat{p}}) \end{bmatrix}$$

where $\boldsymbol{\Phi}_{\hat{p},\hat{p}}^{\rho,\gamma}(\zeta), \boldsymbol{B}_{\hat{p},\hat{p}}^{\eta-\gamma}(\zeta), \boldsymbol{B}_{\hat{p},\hat{p}}^{\eta-1}(\zeta)$ and $\boldsymbol{B}_{\hat{p},\hat{p}}^\eta(\zeta)$ are the operational matrices which are discussed in section (3.2), (3.3) and $\boldsymbol{C}^\rho$ is $1 \times \hat{p}$ matrix. We can solve the equation (3.31), by matrix inversion method for $\boldsymbol{C}^\rho$ and use it in (3.27) to attain $y(\zeta)$ at collocation points.

3.7 Boundary Value Problems

The suggested approach is implemented for Caputo-Hadamard fractional boundary value problems (BVPs) in this section.

Consider the following general form of linear Caputo-Hadamard fractional BVP DE,

$$
\begin{aligned}
&{}^H_\zeta D^\eta_a y(\zeta) + \mu_1(\zeta){}^H_\zeta D^\gamma_a y(\zeta) + \mu_2(\zeta)y(\zeta) = h(\zeta), \\
&a < \zeta \le ae, \quad 1 < \eta \le 2, \quad 0 < \gamma \le 1, \\
&y(a) = \alpha_1, \quad y(ae) = \alpha_2.
\end{aligned} \tag{3.32}
$$

Approximating the higher order term using the Gegenbauer wavelet series, as described in (3.4).

$$
{}^H_\zeta D^\eta_a y(\zeta) = \sum_{m=0}^{2^{k-1}} \sum_{n=0}^{N-1} c^\rho_{m,n} \Phi^{\rho,\gamma}_{m,n}(\zeta) = \mathcal{C}^\rho \Phi^{\rho,\gamma}(\zeta). \tag{3.33}
$$

After Caputo-Hadamard fractional integration of (3.30), and by using the BCs, we get

$$
y(\zeta) = \mathcal{C}^\rho {}_\zeta I^\eta_a \Phi^{\rho,\gamma}(\zeta) - c_1 \ln(\zeta) - c_2. \tag{3.34}
$$

Using the boundary conditions, we have $c_1 = \frac{1}{(\ln(a)-\ln(ae))}\left[C^\rho{}_\zeta I^\eta_a \Phi^{\rho,\gamma}(ae) - (\alpha_1 - \alpha_2)\right]$ and $c_2 = -\alpha_1 - \frac{\ln(a)}{(\ln(a)-\ln(ae))}\left[C^\rho{}_\zeta I^\eta_a \Phi^{\rho,\gamma}(ae) - (\alpha_1 - \alpha_2)\right]$.

$$
\begin{aligned}
y(\zeta) =& \mathcal{C}^\rho {}_\zeta I^\eta_a \Phi^{\rho,\gamma}(\zeta) - \frac{1}{(\ln(a)-\ln(ae))}\left[C^\rho{}_\zeta I^\eta_a \Phi^{\rho,\gamma}(ae) - (\alpha_1 - \alpha_2)\right]\ln(\zeta) \\
&+ \frac{\ln(a)}{(\ln(a)-\ln(ae))}\left[C^\rho{}_\zeta I^\eta_a \Phi^{\rho,\gamma}(ae) - (\alpha_1 - \alpha_2)\right] + \alpha_1,
\end{aligned} \tag{3.35}
$$

and

$$
{}^H_\zeta D^\gamma_a y(\zeta) = \mathcal{C}^\rho {}_\zeta I^{\eta-\gamma}_a \Phi^{\rho,\gamma}(\zeta) - \frac{1}{(\ln(a)-\ln(ae))}\left[C^\rho{}_\zeta I^\eta_a \Phi^{\rho,\gamma}(ae) - (\alpha_1 - \alpha_2)\right]\frac{\Gamma 2}{\Gamma(2-\gamma)}(\ln(\zeta))^{(1-\gamma)}. \tag{3.36}
$$

By substituting equations (3.33), (3.34) and (3.35), in (3.32), we obtain

$$
\mathcal{C}^\rho \left[\Phi^{\rho,\gamma}(\zeta) +{}_\zeta I^{\eta-\gamma}_a \Phi^{\rho,\gamma}(\zeta)A_0 +{}_\zeta I^\eta_a \Phi^{\rho,\gamma}(\zeta)A_1 +{}_\zeta I^\eta_a \Phi^{\rho,\gamma}(ae)A_2\right] = h(\zeta) - \frac{\mu_1(\zeta)(\alpha_1 - \alpha_2)}{(\ln(a)-\ln(ae))}
$$

$$
\frac{\Gamma 2}{\Gamma(2-\gamma)}(\ln(\zeta))^{(1-\gamma)} - \frac{\mu_2(\zeta)(\alpha_1 - \alpha_2)}{(\ln(a)-\ln(ae))}(\ln(\zeta)) + \frac{ln(a)}{(\ln(a)-\ln(ae))}\mu_2(\zeta)(\alpha_1 - \alpha_2)(\ln(\zeta)), \tag{3.36}
$$

where

$$
\begin{aligned}
\mathcal{R} =& h(\zeta) - \frac{\mu_1(\zeta)(\alpha_1 - \alpha_2)}{(\ln(a)-\ln(ae))}\frac{\Gamma 2}{\Gamma(2-\gamma)(\ln(\zeta))^{(1-\gamma)}} - \frac{\mu_2(\zeta)(\alpha_1 - \alpha_2)}{(\ln(a)-\ln(ae))}(\ln(\zeta)) \\
&+ \frac{\ln(a)}{(\ln(a)-\ln(ae))}\mu_2(\zeta)(\alpha_1 - \alpha_2)(\ln(\zeta)).
\end{aligned}
$$

Expanding equation (3.36) at collocation points, $\zeta_i = \frac{ae^{2i-1}}{2^{\hat{p}}}, i = 1, 2, \ldots, \hat{p}$, we have

$$
\boldsymbol{C}^\rho \left[\boldsymbol{\Phi}^{\rho,\gamma}_{\hat{p},\hat{p}}(\zeta) + \boldsymbol{B}^{\rho,\eta-\gamma}_{\hat{p},\hat{p}}(\zeta)A_0 + \boldsymbol{B}^{\rho,\eta}_{\hat{p},\hat{p}}(\zeta)A_1 + \boldsymbol{Q}^{\rho,\eta}_{\hat{p},\hat{p}}(\zeta)A_2\right] = \boldsymbol{\mathcal{R}}_{1\times\hat{p}}. \tag{3.37}
$$

The vector $\boldsymbol{R}_{1\times\hat{p}} = \left[\mathcal{R}(\zeta 1), \mathcal{R}(\zeta_2), \ldots, \mathcal{R}(\zeta_{\hat{p}}) \right]$ is known, and the matrices A_0, A_1, and A_2 are diagonal matrices of order $\hat{p} \times \hat{p}$, given by

$$
A_0 = \begin{bmatrix} a_0(\zeta_1) & 0 & \cdots & 0 \\ 0 & a_0(\zeta_2) & \cdots & 0 \\ \vdots & \vdots & \ddots & \vdots \\ 0 & 0 & \cdots & a_0(\zeta_{\hat{p}}) \end{bmatrix}, A_1 = \begin{bmatrix} a_1(\zeta_1) & 0 & \cdots & 0 \\ 0 & a_1(\zeta_2) & \cdots & 0 \\ \vdots & \vdots & \ddots & \vdots \\ 0 & 0 & \cdots & a_1(\zeta_{\hat{p}}) \end{bmatrix}
$$

and

$$
A_2 = \begin{bmatrix} a_2(\zeta_1) & 0 & \cdots & 0 \\ 0 & a_2(\zeta_2) & \cdots & 0 \\ \vdots & \vdots & \ddots & \vdots \\ 0 & 0 & \cdots & a_2(\zeta_{\hat{p}}) \end{bmatrix}.
$$

The operational matrices $\boldsymbol{\Phi}_{\hat{p},\hat{p}}^{\rho,\gamma}(\zeta)$, $\boldsymbol{B}_{\hat{p},\hat{p}}^{\rho,\eta-\gamma}(\zeta)$, $\boldsymbol{B}_{\hat{p},\hat{p}}^{\rho,\eta}(\zeta)$, and $\boldsymbol{Q}_{\hat{p},\hat{p}}^{\rho,\eta}(\zeta)$, as detailed in the referenced section (3.2), (3.3) and (3.4) along with the $1 \times \hat{p}$ matrix $\boldsymbol{C}^\rho$, are used to solve equation (3.37). By employing the matrix inversion method to solve for $\boldsymbol{C}^\rho$, we can then substitute this solution into equation (3.34) to determine $y(\zeta)$ at the collocation points.

3.8   Numerical Results and Discussion

This section shows how the present numerical technique, which is based on fractional integration operational matrices for Hadamard Gegenbauer wavelets, is implemented by taking two examples.

Example 1. A linear IVP Caputo-Hadamard fractional differential equation with variable coefficient is considered as,

$$
{}_\zeta^H D_a^\eta y(\zeta) + \mu_1(\zeta) {}_\zeta^H D_a^1 y(\zeta) + \mu_2(\zeta) y(\zeta) = g(\zeta), \quad 1 < \eta \leq 2, \quad 1 < \zeta < e. \tag{3.38}
$$

Initial conditions

$$
y(1) = 0, \quad {}_\zeta^H D^1 y(1) = 0,
$$

where $\mu_1(\zeta) = cos(\zeta) + 2\zeta^2$ and $\mu_2(\zeta) = \ln(\zeta)$. In this case function $g(\zeta) = \frac{\Gamma(\kappa+2)}{\Gamma(2+\kappa-\eta)}(\ln(\zeta))^{1+\kappa-\eta} + \mu_1(\zeta)\frac{\Gamma(\kappa+2)}{\Gamma(1+\kappa)}(\ln(\zeta))^\kappa + \mu_2(\zeta)ln(\zeta))^{\kappa+1}$, and exact solution is $y(\zeta) = (\ln(\zeta))^{\kappa+1}$. After applying the Hadamard Gegenbauer wavelets method to (3.38), we obtain

$$
\mathcal{C}^\rho \left(\Phi^{\rho,\gamma}(\zeta) + {}_\zeta I_a^{\eta-1} \Phi^{\rho,\gamma}(\zeta)\mu_1(\zeta) + {}_\zeta I_a^\eta \Phi^{\rho,\gamma}(\zeta)\mu_2(\zeta) \right) = \mathcal{G}, \tag{3.39}
$$

where $\Phi^{\rho,\gamma}(\zeta)$, ${}_\zeta I_a^{\eta-1} \Phi^{\rho,\gamma}(\zeta)$ and ${}_\zeta I_a^\eta \Phi^{\rho,\gamma}(\zeta)$ are operational matrices, $\mathcal{G} = \left[g(\zeta_1), g(\zeta_2), \ldots, g(\zeta_{\hat{p}}) \right]$ is $1 \times \hat{p}$ matrix and $\mu_1(\zeta), \mu_2(\zeta)$ is diagonal matrix. We solve the above equation (3.39) for $\mathcal{C}^\rho$ and substitute it in equation (3.38) to get $y(\zeta)$ at collocation points. After utilizing the collocation points, the solution is given as

$$
\mathbf{y} = \mathcal{C}^\rho {}_\zeta I_a^\eta \Phi^{\rho,\gamma}(\zeta), \tag{3.40}
$$

31
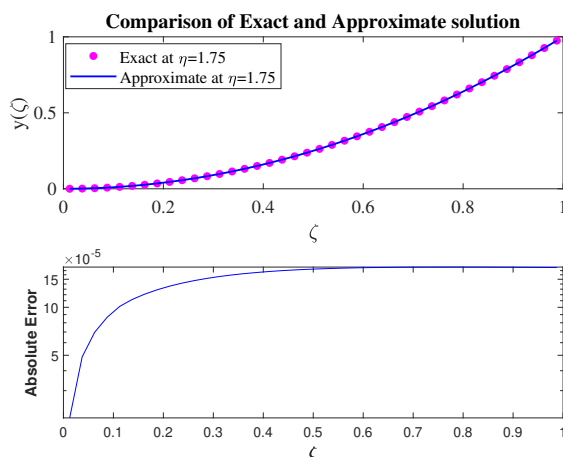
Figure 3.1: The approximate and exact solution for $\eta = 1.75$ when $M = 4$ & $k = 3$.

Figure 3.2: Numerical solution by choosing $\eta \in [1.70, 1.90]$ when $k = 4$ & $M = 5$
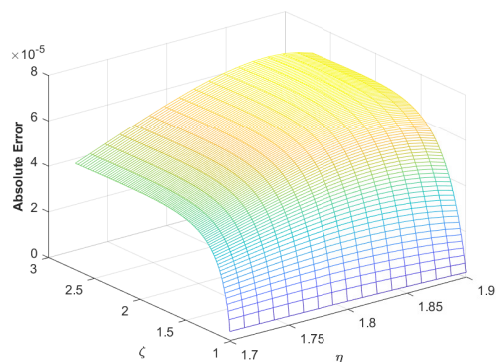
Figure 3.3: Absolute errors by choosing $\eta \in [1.70, 1.90]$ when $k = 4$ & $M = 5$

where $y = [y(\zeta_1), y(\zeta_2), ..., y(\zeta_{\bar{p}})]$.

In Figure 3.1, the proposed scheme's approximate solution is represented by a dotted line, while the exact solution, obtained by selecting $k = 3$, $M = 4$, and $\eta = 1.75$, is shown by a solid line. Figures 3.2 and 3.3 show the graphs for the approximate solution and absolute errors, respectively, for varying η within the range $[1.70, 1.90]$, with $k = 4$ and $M = 5$. Table 3.1 provides the absolute error for various combinations of k and M. It is evident that increasing k and M values while maintaining η constant results in a reduction in error.

Example 2. Consider the following boundary value problem (BVP) involving the Caputo-Hadamard fractional derivative.

$$_{\zeta}^{H}D_a^{\eta}y(\zeta) + e_1(\zeta)_{\zeta}^{H}D_a^{\gamma}y(\zeta) + e_2(\zeta)y(\zeta) = f(\zeta), \quad 1 < \eta \leq 2, \quad 0 < \gamma < 1. \tag{3.41}$$

Boundary conditions.

32

Table 3.1. The current scheme's absolute errors at a constant η vary with different choices of k and M.

$\eta = 1.2$	$M = 2, k = 3$	$M = 3, k = 4$	$M = 5, k = 6$	$M = 6, k = 6$
ζ	$\mathbb{E}_{abs}$	$\mathbb{E}_{abs}$	$\mathbb{E}_{abs}$	$\mathbb{E}_{abs}$
0	$7.9565e-05$	$5.1516e-06$	$1.1343e-07$	$7.6368e-08$
0.2	$6.7067e-05$	$6.5223e-06$	$1.8506e-07$	$1.1916e-07$
0.4	$9.1782e-05$	$6.7561e-06$	$1.8028e-07$	$1.1238e-07$
0.6	$9.2381e-05$	$6.7457e-06$	$1.6906e-07$	$9.9450e-08$
0.8	$9.1114e-05$	$6.6763e-06$	$1.5118e-07$	$7.7517e-08$
1	$9.0910e-05$	$6.5983e-06$	$1.4254e-07$	$7.0908e-08$

$$y(1) = 0, \quad y(e) = 1.$$

For $e_1(\zeta) = \ln(\zeta)$ and $e_2(\zeta) = \sin(\zeta)$, $f(\zeta) = \frac{\Gamma(\kappa+1)}{\Gamma(1+\kappa-\eta)}(\log(\zeta))^{\kappa-\eta} + e_1(\zeta)\frac{\Gamma(\kappa+1)}{\Gamma(1+\kappa-\gamma)}(\log(\zeta))^{\kappa-\gamma} + e_2(\zeta)\ln(\zeta))^{\kappa}$, The exact solution is given by $y(\zeta) = (\ln(\zeta))^{\kappa}$. Figures 3.4 and 3.5 display the graphs for the approximate solution and absolute errors, respectively, for varying η within the range $[1.75, 1.95]$, with $k = 4$ and $M = 5$. By selecting different values for η and γ, and fixing $k = 3$ and $M = 4$, both exact and approximate solutions, along with their absolute errors are plotted in Figure 3.6. This illustrates different errors at various orders. The absolute errors provided in Table 3.2, it can be reduced by increasing k and M values.
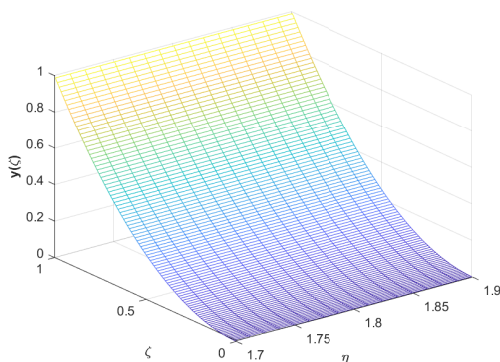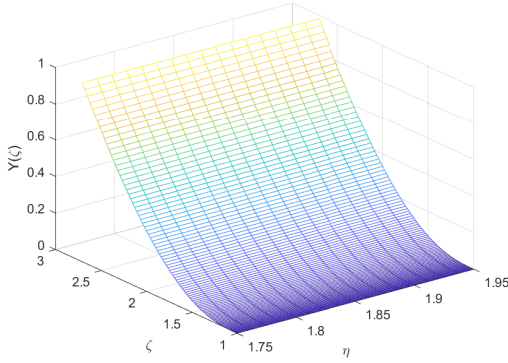

Figure 3.4: Numerical solution by choosing $\eta \in [1.75, 1.95]$ when $k = 4$ & $M = 5$
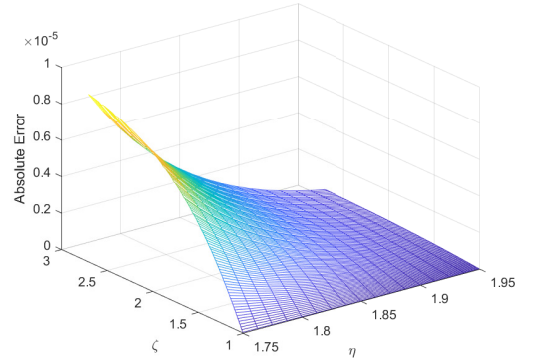
Figure 3.5: Absolute errors by choosing $\eta \in [1.75, 1.95]$ when $k = 4$ & $M = 5$

Table 3.2. The current scheme's absolute errors at a constant η and γ vary with different choices of k and M.

$\eta = 1.9, \gamma = 0.2$	$M = 3, k = 2$	$M = 4, k = 3$	$M = 5, k = 4$	$M = 6, k = 5$
ζ	$\mathbb{E}_{abs}$	$\mathbb{E}_{abs}$	$\mathbb{E}_{abs}$	$\mathbb{E}_{abs}$
0	$2.5548\mathrm{e}-06$	$3.0013\mathrm{e}-07$	$4.2945\mathrm{e}-08$	$5.2131\mathrm{e}-09$
0.2	$2.0041\mathrm{e}-05$	$4.8707\mathrm{e}-06$	$1.6790\mathrm{e}-06$	$4.6841\mathrm{e}-07$
0.4	$3.2651\mathrm{e}-05$	$9.3996\mathrm{e}-06$	$2.9654\mathrm{e}-06$	$8.3860\mathrm{e}-07$
0.6	$3.8315\mathrm{e}-05$	$1.1611\mathrm{e}-05$	$3.5139\mathrm{e}-06$	$9.9142\mathrm{e}-07$
0.8	$3.4037\mathrm{e}-05$	$9.8320\mathrm{e}-06$	$3.0032\mathrm{e}-06$	$8.3546\mathrm{e}-07$
1	$1.8673\mathrm{e}-05$	$5.0044\mathrm{e}-06$	$1.3531\mathrm{e}-06$	$3.6485\mathrm{e}-07$
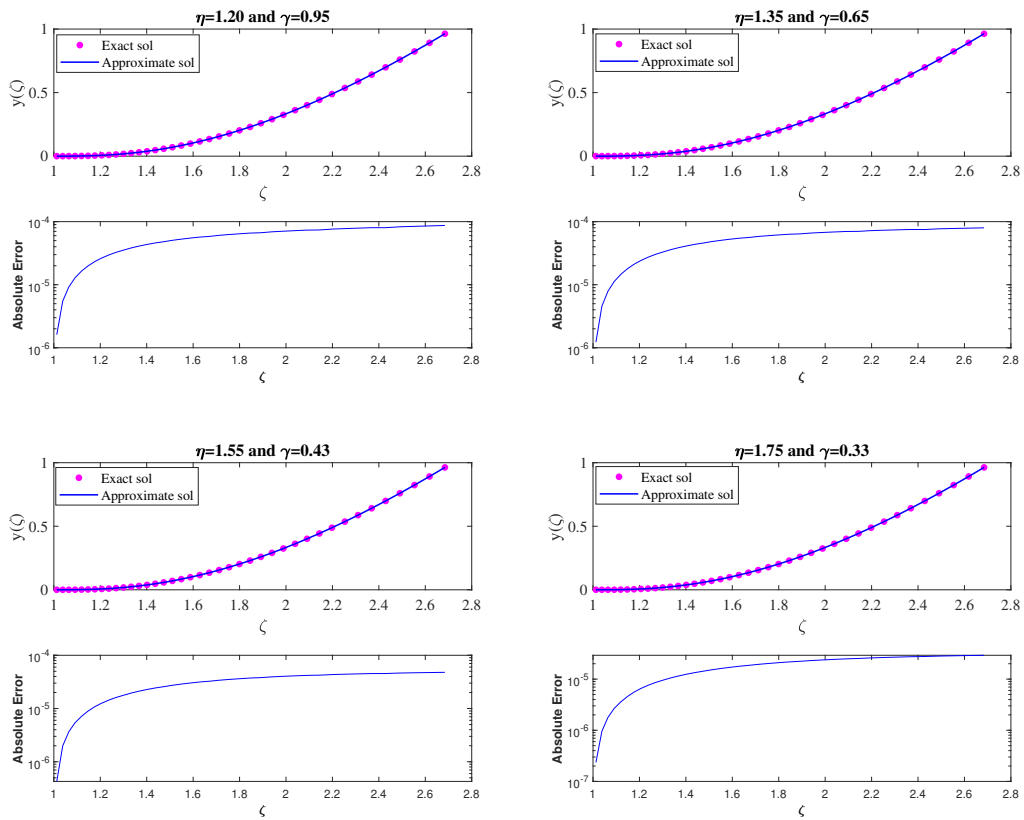
Figure 3.6: Exact solutions and solutions generated by hadamard Gegebauer Wavelet scheme for $k = 3$ and $M = 4$, at different orders.

3.9 Conclusion

The Caputo-Hadamard Gegenbauer wavelets method has proven to perform well when used to solve various fractional initial value problems (IVPs) and boundary value problems (BVPs). Numerical solutions of these problems converged to the exact solutions by increasing the values of k and M. From the numerical examples, it is shown that the Caputo-Hadamard Gegenbauer wavelets technique is capable of addressing a variety of fractional order differential equations effectively, providing good results.

Chapter 4

Fast Haar Wavelets Method

The Haar wavelet method is now a key tool for solving both initial value problems (IVPs) and boundary value problems (BVPs) involving Caputo fractional differential equations and Caputo partial fractional differential equations. Researchers have made important advancements in this area by developing efficient and accurate methods that take advantage of the unique features of Haar wavelets. The ψ-Haar wavelets method [51] has been created to extend its use to nonlinear fractional differential equations using a technique called quasi-linearization. This method has shown high accuracy and efficiency in various numerical examples, making it useful for solving both linear and nonlinear fractional differential equations. Jafari has made significant contributions to this field by applying Haar wavelets to solve fractional differential equations. For example, his work on using Haar wavelet operational matrices to solve generalized Caputo-Katugampola fractional differential equations has shown better accuracy and efficiency. This approach works well for generalized fractional boundary value problems [52], proving to be more effective than previous methods. Haar wavelet methods combined with Green's functions have also been used to solve partial differential equations of arbitrary order, showing better accuracy than standard Haar wavelet methods. This combined method has successfully solved complex equations like nonlinear Burger's equations [53]. Zhang et al, [54] introduced a fast Euler-Maruyama method for nonlinear fractional stochastic differential equations, which improves computational efficiency and achieves strong convergence. Their method uses a sum-of-exponentials approximation and has been effective in numerical tests. Additionally, Jiang et al. [44] showed how fast evaluation methods for Caputo fractional derivatives work well in fractional diffusion equations, highlighting the potential of these techniques to improve numerical solutions of PDEs. Fast evaluation methods, known for their speed and accuracy, enhance the Haar wavelet approach by speeding up the numerical solution process. This combination offers the potential for significant improvements in the numerical treatment of complex fractional models, providing powerful tools for engineers and scientists.

4.1   Haar wavelet

The father and mother wavelets [48] for the Haar wavelet family are defined as,

$$\mathbf{\Phi}_0(\tau) = \begin{cases} 1, & 0 \le \tau < 1, \\ 0, & \text{otherwise,} \end{cases} \tag{4.1}$$

$$\mathbf{\Phi}_1(\tau) = \begin{cases} 1, & 0 \le \tau < \frac{1}{2}, \\ -1, & \frac{1}{2} \le \tau < 1, \\ 0, & \text{otherwise.} \end{cases} \tag{4.2}$$

According to. With the help of integer translations and dyadic dilations of the mother wavelet Φ_1, the other functions in the family of Haar wavelets are produced as follows:

$$\mathbf{\Phi}_i(\tau) = \begin{cases} 2^j, & \rho_1(i) \le \tau \le \rho_2(i), \\ -2^j, & \rho_2(i) \le \tau \le \rho_3(i), \\ 0, & \text{otherwise.} \end{cases} \tag{4.3}$$

Let $\rho_1(i) = \frac{k}{m}$, $\rho_2(i) = \frac{k+0.5}{m}$, and $\rho_3(i) = \frac{k+1}{m}$, where $i = 2^j + k + 1$, $j = 0, 1, 2, \cdots, J$ represent the dilation parameter. Here, $m = 2^j$ and $k = 0, 1, 2, \cdots, 2^j - 1$ are the translation parameters. While J stands for the maximal level of resolution. The Haar wavelets' collocation points are typically denoted as $\tau_j = \frac{j-0.5}{m}$, where $j = 1, 2, \ldots, m$.

4.2   Integral of Haar Wavelets

We find the integrals of the Haar function. By integrating the Haar function γ times, we obtain

$$\boldsymbol{P}_{\gamma,i}(\tau) = \frac{2^j}{(\gamma-1)!} \int_a^\tau (\tau - s)^{\gamma-1} \mathbf{\Phi}_i(s) ds. \tag{4.4}$$

These integrals can generally be evaluated using equation (4.1). If $\tau \in [\rho_1, \rho_2)$ then, based on equation (4.3), we have the following:

$$\boldsymbol{P}_{\gamma,i}(\tau) = \frac{2^j}{(\gamma-1)!} \int_{\rho_1(i)}^\tau (\tau - s)^{\gamma-1} \mathbf{\Phi}_i(s) ds = \frac{2^j}{\gamma!} \left[\tau - \rho_1(i)\right]^\gamma.$$

If $\tau \in [\rho_2, \rho_3)$,

$$\begin{aligned} \boldsymbol{P}_{\gamma,i}(\tau) &= \frac{2^j}{(\gamma-1)!} \int_{\rho_1(i)}^\tau (\tau - s)^{\gamma-1} \mathbf{\Phi}_i(s) ds, \\ &= \frac{2^j}{(\gamma-1)!} \left[\int_{\rho_1(i)}^{\rho_2(i)} (\tau - s)^{\gamma-1} \mathbf{\Phi}_i(s) ds + \int_{\rho_2(i)}^\tau (\tau - s)^{\gamma-1} \mathbf{\Phi}_i(s) ds \right], \\ &= \frac{2^j}{\gamma!} \left\{ \left[\tau - \rho_1(i)\right]^\gamma - 2\left[\tau - \rho_2(i)\right]^\gamma \right\}. \end{aligned}$$

37

If $\tau \geq \rho_3(i)$,

$$
\begin{aligned}
\boldsymbol{P}_{\gamma,i}(\tau) &= \frac{2^j}{(\gamma-1)!} \int_{\rho_1(i)}^{\tau} (\tau-s)^{\gamma-1}\boldsymbol{\Phi}_i(s)ds, \\
&= \frac{2^j}{(\gamma-1)!} \left[\int_{\rho_1(i)}^{\rho_2(i)} (\tau-s)^{\gamma-1}\boldsymbol{\Phi}_i(s)ds + \int_{\rho_2(i)}^{\rho_3(i)} (\tau-s)^{\gamma-1}\boldsymbol{\Phi}_i(s)ds \right. \\
&\quad \left. + \int_{\rho_3(i)}^{\tau} (\tau-s)^{\gamma-1}\boldsymbol{\Phi}_i(s)ds \right], \\
&= \frac{2^j}{\gamma!} \left\{ [\tau-\rho_1(i)]^{\gamma} - 2[\tau-\rho_2(i)]^{\gamma} + [\tau-\rho_3(i)]^{\gamma} \right\}.
\end{aligned}
$$

Therefore, the integrals of the Haar wavelet functions of order γ in equation (4.2) can be expressed as,

$$
\boldsymbol{P}_{\gamma,i}(\tau) = \begin{cases}
0, & \text{for } \tau < \rho_1(i), \\
\frac{2^j}{\gamma!}[\tau-\rho_1(i)]^{\gamma}, & \text{for } \tau \in [\rho_1(i), \rho_2(i)], \\
\frac{2^j}{\gamma!}\left\{[\tau-\rho_1(i)]^{\gamma} - 2[\tau-\rho_2(i)]^{\gamma}\right\}, & \text{for } \tau \in [\rho_2(i), \rho_3(i)], \\
\frac{2^j}{\gamma!}\left\{[\tau-\rho_1(i)]^{\gamma} - 2[\tau-\rho_2(i)]^{\gamma} + [\tau-\rho_3(i)]^{\gamma}\right\}, & \text{for } \tau > \rho_3(i).
\end{cases} \tag{4.5}
$$

Above equation (4.5) hold for $i > 1$. For the case $i = 1$ we have $\rho_1(1) = \rho_1$, $\rho_2(1) = \rho_3(1) = \rho_2$ and

$$
\boldsymbol{P}_{\gamma,1}(\tau) = \frac{2^j}{\gamma!}(\tau-\rho_1)^{\gamma}, \tag{4.6}
$$

4.3 Function Approximation by the Haar Wavelets

The function $y(\tau)$ is defined on the interval, it can be decomposed in terms of the haar wavelet as follows,

$$
y(\tau) = \sum_{i=1}^{\infty} C_i \Phi_i(\tau), \tag{4.7}
$$

with i as an integer index for the finite or infinite sum, where $\boldsymbol{C}_i$ represents the Haar wavelet coefficient and $\Phi_i(\tau)$ are the basis functions, let us consider the first m.

$$
y_M(\tau) = \sum_{i=1}^{m} C_i \Phi_i(\tau), i = 2^j + k + 1, j = 0, 1, 2, \ldots, J, k = 0, 1, 2, \ldots, 2^j - 1. \tag{4.8}
$$

The approximation function defined as $y_M(xi)$,

$$
y_M(\tau_i) = \sum_{i=1}^{m} \boldsymbol{C}_i \boldsymbol{\Phi}_i(\tau_i). \tag{4.8}
$$

Equation (4.8) in matrix form.

$$
y = \boldsymbol{C\Phi}, \tag{4.9}
$$

where $\mathbf{C} = \begin{bmatrix} C_1 & C_2 & \cdots & C_m \end{bmatrix}$ and $\mathbf{y} = \begin{bmatrix} y_1 & y_2 & \cdots & y_m \end{bmatrix}$ are row vactors of m dimensional and

$$\boldsymbol{\Phi}_{m \times m} = \begin{bmatrix} \Phi_1\left(x_{(}1)\right) & \Phi_1\left(x(2)\right) & \cdots & \Phi_1\left(x(m)\right) \\ \Phi_2\left(x(1)\right) & \Phi_2\left(x(2)\right) & \cdots & \Phi_2\left(x(m)\right) \\ \vdots & \vdots & \ddots & \vdots \\ \Phi_m\left(x(1)\right) & \Phi_m\left(x(2)\right) & \cdots & \Phi_m\left(x(m)\right) \end{bmatrix}.$$

In particular, for $J = 3$, we get $m = 8$ and the Haar matrix is given as,

$$\boldsymbol{\Phi}_{8 \times 8} = \begin{bmatrix} 1 & 1 & 1 & 1 & 1 & 1 & 1 & 1 \\ 1 & 1 & 1 & 1 & -1 & -1 & -1 & -1 \\ 1 & 1 & -1 & -1 & 0 & 0 & 0 & 0 \\ 0 & 0 & 0 & 0 & 1 & 1 & -1 & -1 \\ 1 & -1 & 0 & 0 & 0 & 0 & 0 & 0 \\ 0 & 0 & 1 & -1 & 0 & 0 & 0 & 0 \\ 0 & 0 & 0 & 0 & 1 & -1 & 0 & 0 \\ 0 & 0 & 0 & 0 & 0 & 0 & 1 & -1 \end{bmatrix},$$

with $\boldsymbol{C}$ determined by,

$$\boldsymbol{C} = \boldsymbol{y}[\boldsymbol{\Phi}]^{-1}, \tag{4.10}$$

where $\boldsymbol{\Phi}^{-1}$ is the inverse of $\boldsymbol{\Phi}$ and equation (4.10) gives the Haar coefficients C_i which are used in (4.7) to get the solution $y(x)$. Among various methods to evaluate the error function of the wavelet estimations, one such error function is defined as follows:

$$E = \int_0^1 [y(\tau) - y_M(\tau)]^2 d\tau. \tag{4.11}$$

Within the class of piecewise functions are the Haar wavelets. The rate of convergence for the piecewise constant function is shown to be $O\left(\frac{1}{M^2}\right)$, provided that the function is sufficiently smooth.

4.4   Fractional Integration Operational Matrix of Haar Wavelet

The defined infinite series can be used to approximate the function $y(\tau)$,

$$y(\tau) = \sum_{i=0}^{\infty} \boldsymbol{C}_i \Phi_i(\tau), \tag{4.12}$$

with taking first m-terms of above (4.12) equation,

$$y_M(\tau) = \sum_{i=0}^{m} \boldsymbol{C}_i \boldsymbol{\Phi}_i(\tau), \tag{4.13}$$

by substituting the collocation points into equation (4.13), we have

$$y_M\left(\tau_i\right) = \sum_{i=0}^{m} \boldsymbol{C}_i \boldsymbol{\Phi}_i\left(\tau_i\right),$$

by applying the integral, we obtain

$$_\tau \mathbb{I}_{\rho_1}^\gamma y_M(\tau) = \boldsymbol{C}_m {}_\tau \mathbb{I}_{\rho_1}^\gamma \boldsymbol{\Phi}_m(x) = \boldsymbol{C}_m \boldsymbol{P}_{m \times m}^\gamma \boldsymbol{\Phi}_m(\tau). \tag{4.14}$$

We used equations (4.5) and (4.6) to compute $_x\mathbb{I}_{\rho_1}^\gamma \mathbf{\Phi}_m(x) = \boldsymbol{P}_{m \times m}^\gamma \mathbf{\Phi}_m(x)$. The expression in equation (4.14) represents the required fractional integral of $y_M(x)$ using Haar wavelets.

$$
\mathbf{P}_{m \times m} = \begin{bmatrix}
p_{\gamma,1}\left(\tau(1)\right) & p_{\gamma,1}\left(\tau(2)\right) & \cdots & p_{\gamma,1}\left(\tau(m)\right) \\
p_{\gamma,2}\left(x(1)\right) & p_{\gamma,2}\left(\tau(2)\right) & \cdots & p_{\gamma,2}\left(\tau(m)\right) \\
\vdots & \vdots & \ddots & \vdots \\
p_{\gamma,m}\left(\tau(1)\right) & p_{\gamma,m}\left(\tau(2)\right) & \cdots & p_{\gamma,m}\left(\tau(m)\right)
\end{bmatrix}.
$$

In particular, we fix $J = 3$ and $\gamma = 0.95$, resulting in $m = 8$. The Haar wavelet operational matrix of fractional integration is.

$$
\mathbf{P}_{8 \times 8} = \begin{bmatrix}
0.0733 & 0.2081 & 0.3380 & 0.4653 & 0.5908 & 0.7149 & 0.8378 & 0.9598 \\
0.0733 & 0.2081 & 0.3380 & 0.4653 & 0.4443 & 0.2988 & 0.1618 & 0.0292 \\
0.1036 & 0.2942 & 0.2708 & 0.0696 & -0.0169 & -0.0109 & -0.0081 & -0.0065 \\
0 & 0 & 0 & 0 & 0.1036 & 0.2942 & 0.2708 & 0.0696 \\
0.1465 & 0.1230 & -0.0097 & -0.0053 & -0.0037 & -0.0028 & -0.0023 & -0.0019 \\
0 & 0 & 0.1465 & 0.1230 & -0.0097 & -0.0053 & -0.0037 & -0.0028 \\
0 & 0 & 0 & 0 & 0.1465 & 0.1230 & -0.0097 & -0.0053 \\
0 & 0 & 0 & 0 & 0 & 0 & 0.1465 & 0.1230
\end{bmatrix}.
$$

4.5 Operational Matrix of Fractional Integration with Haar Wavelet for Boundary Value Problems

The fractional integral is applied to obtain another operational matrix, which helps us solve the fractional boundary value problem[50]. Suppose that $[0, \eta]$ is the compact support of Haar functions and that $f : [0, \eta] \to \mathbb{R}$ is a continuous function with $\eta > 0$.

$$
I_0^\gamma \Phi_1(\eta) = 2^j \int_0^\eta (\eta - s)^{\gamma - 1} ds, \tag{4.15}
$$

by simplifying,

$$
f(\tau) I_0^\gamma \Phi_1(\eta) = f(\tau) \frac{2^j \eta^\gamma}{\Gamma(\gamma + 1)}. \tag{4.16}
$$

By assigning $C_{\gamma,l} = \frac{2^j \eta^\gamma}{\Gamma(\gamma+1)}$,

$$
s^{\gamma, \eta, 1} = f(\tau) C_{\gamma, 1}, \tag{4.17}
$$

and

$$
f(\tau) I_0^\gamma \Phi_i(\eta) = 2^j f(\tau) \left[\int_{\rho_1(i)}^{\rho_2(i)} (\eta - s)^{\gamma - 1} ds - \int_{\rho_2(i)}^{\rho_3(i)} (\eta - s)^{\gamma - 1} ds \right], \tag{4.18}
$$

$$
f(\tau) I_0^\gamma \Phi_i(\eta) = f(\tau) \frac{2^j}{\Gamma(\gamma + 1)} \left[(\eta - \rho_1(i))^\gamma - 2(\eta - \rho_2(i))^\gamma + (\eta - \rho_3(i))^\gamma \right], \tag{4.19}
$$

$$C_{\gamma,i} = \frac{2^j}{\Gamma(\gamma+1)} \left[(\eta - \rho_1(i))^\gamma - 2(\eta - \rho_2(i))^\gamma + (\eta - \rho_3(i))^\gamma \right],$$

$$s^{\gamma,\eta,i} = f(\tau)C_{\gamma,i}. \tag{4.20}$$

For $s^{\gamma,\eta,1} = f(\tau)I_0^\gamma \Phi_1(\eta)$ and $s^{\gamma,\eta,i} = f(x)I_0^\gamma \Phi_i(\eta)$, where $i = 2^j + k + 1$, $j = 0, 1, 2, \cdots, J$, and $k = 0, 1, 2, \cdots, 2^j - 1$, let $\tau(i) = \frac{i-0.5}{m}, i = 1, 2, \cdots, m$. Define a matrix $\mathbf{S}$ using the collocation points τ as described in (4.19) and (4.20).

$$\mathbf{S}_{\mathbf{m}\times\mathbf{m}}^{\gamma,\eta} = \begin{bmatrix} f\left(\tau(1)\right)I_0^\gamma\Phi_1(\eta) & f\left(\tau(2)\right)I_0^\gamma\Phi_1(\eta) & \cdots & f\left(\tau(m)\right)I_0^\gamma\Phi_1(\eta) \\ f\left(\tau(1)\right)I_0^\gamma\Phi_2(\eta) & f\left(\tau(2)\right)I_0^\gamma\Phi_2(\eta) & \cdots & f\left(\tau(m)\right)I_0^\gamma\Phi_2(\eta) \\ \vdots & \vdots & \ddots & \vdots \\ f\left(\tau(1)\right)I_0^\gamma\Phi_m(\eta) & f\left(\tau(2)\right)I_0^\gamma\Phi_m(\eta) & \cdots & f\left(\tau(m)\right)I_0^\gamma\Phi_m(\eta) \end{bmatrix}.$$

In particular, for $\eta = 1, 25, f(\tau) = cos(\tau), \gamma = 0.25, J = 3$, we get

$$\mathbf{S}_{\mathbf{8}\times\mathbf{8}}^{1.25,1} = \begin{bmatrix} 1.1011 & 1.0839 & 1.0498 & 0.9994 & 0.9333 & 0.8526 & 0.7587 & 0.6529 \\ -0.7507 & -0.7390 & -0.7158 & -0.6813 & -0.6363 & -0.5813 & -0.5173 & -0.4452 \\ -0.0316 & -0.0311 & -0.0302 & -0.0287 & -0.0268 & -0.0245 & -0.0218 & -0.0188 \\ -0.8928 & -0.8788 & -0.8512 & -0.8103 & -0.7567 & -0.6913 & -0.6151 & -0.5294 \\ -0.0082 & -0.0081 & -0.0078 & -0.0075 & -0.0070 & -0.0064 & -0.0057 & -0.0049 \\ -0.0149 & -0.0147 & -0.0142 & -0.0135 & -0.0127 & -0.0116 & -0.0103 & -0.0089 \\ -0.0376 & -0.0370 & -0.0359 & -0.0341 & -0.0319 & -0.0291 & -0.0259 & -0.0223 \\ -1.0617 & -1.0451 & -1.0122 & -0.9636 & -0.8999 & -0.8221 & -0.7315 & -0.6295 \end{bmatrix}.$$

The Haar matrices $\mathbf{\Phi}$, $\mathbf{P}$, and $\mathbf{S}$ are formulated for addressing initial and boundary value problems involving fractional orders.

4.6   Error analysis

In this section, we explain an inequality in [49]. This inequality provides an upper bound, demonstrating the convergence of the Haar wavelet technique.

Theorem 3.1.1. Suppose that we have differentiable function $y(\tau)$ and its first derivative is bounded by $M > 0$ on the interval $(0,1)$ that is, $\left|y'(\tau)\right| \leq M$; for all $\tau \in (0,1)$, and $y_m(\tau)$ is the approximation of $y(\tau)$. Then we have

$$\left\|y(\tau) - y_m(\tau)\right\| = O\left(\frac{1}{m}\right).$$

Proof. As the function $y(\tau)$, which is defined over $[0,1)$ can be expressed as,

$$y(\tau) = \sum_{i=0}^{\infty} C_i \Phi_i(\tau), \tag{4.21}$$

where $C_i = < y(\tau), \Phi_i(\tau) >$. Let us consider the first m-terms of the above equation (4.21), which is denoted by $y_m(\tau)$ and is the approximation of the function $y(\tau)$, that is

$$y(\tau) \cong y_m(\tau) = \sum_{i=0}^{m} C_i \Phi_i(\tau), \tag{4.22}$$

where, $m = 2^j$, $\quad j = 0, 1, 2, 3, \cdots$. So the difference becomes,

$$y(\tau) - y_m(\tau) = \sum_{i=0}^{\infty} \boldsymbol{C}_i \boldsymbol{\Phi}_i(\tau) - \sum_{i=0}^{m} \boldsymbol{C}_i \boldsymbol{\Phi}_i(\tau), \tag{4.23}$$

$$= \sum_{i=m}^{\infty} \boldsymbol{C}_i \boldsymbol{\Phi}_i(\tau).$$

Taking norm of equation (4.23), we have

$$\left\| y(\tau) - y_m(\tau) \right\|^2 = \int_0^1 \left(y(\tau) - y_m(\tau) \right)^2 dx,$$

$$= \int_0^1 \left(\sum_{i=m}^{\infty} \boldsymbol{C}_i \boldsymbol{\Phi}_i(\tau) \right)^2 d\tau,$$

$$= \sum_{i=m}^{\infty} \sum_{i=m'}^{\infty} \boldsymbol{C}_i \boldsymbol{C}_i \int_0^1 \boldsymbol{\Phi}_i(\tau) \boldsymbol{\Phi}_i(\tau) d\tau. \tag{4.24}$$

By using orthogonality condition, (4.24) becomes,

$$\left\| y(\tau) - y_m(\tau) \right\|^2 = \sum_{i=m}^{\infty} C_i^2 = \sum_{i=2^j}^{\infty} C_i^2, \tag{4.25}$$

where $\boldsymbol{C}_i = <y(\tau), \boldsymbol{\Phi}_i(\tau)> = \int_0^1 y(\tau) \boldsymbol{\Phi}_i(\tau) d\tau$. Since

$$\Phi_i(\tau) = 2^{\frac{j}{2}} \begin{cases} 1, & \text{for } \tau \in \left[k2^{-j}, (k+0.5)2^{-j} \right], \\ -1, & \text{for } \tau \in \left[(k+0.5)2^{-j}, (k+1)2^{-j} \right], \\ 0, & \text{otherwise}, \end{cases}$$

by substituting, we obtained

$$\boldsymbol{C}_i = 2^{\frac{j}{2}} \left\{ \int_{k2^{-j}}^{(k+0.5)2^{-j}} y(\tau) d\tau - \int_{(k+0.5)2^{-j}}^{(k+1)2^{-j}} y(\tau) d\tau \right\}.$$

By mean value theorm, there exit ξ, η in such a way that

$$k2^{-j} \leq \xi < (k+0.5)2^{-j}, \quad (k+0.5)2^{-j} \leq \eta < (k+1)2^{-j}.$$

Therefore

$$\boldsymbol{C}_i = 2^{\frac{j}{2}} \left\{ \left((k+0.5)2^{-j} - \left(k2^{-j} \right) \right) y(\xi) - \left((k+1)2^{-j} \right. \right. \tag{4.26}$$

$$\left. \left. - \left((k+0.5)2^{-j} \right) \right) y(\eta) \right\}.$$

After simplifying equation (4.26), we obtained

$$\boldsymbol{C}_i = 2^{\frac{j}{2}-j-1}(y(\xi) - y(\eta)),$$

42

$$C_i = 2^{\frac{-j}{2}-1}(\eta - \xi)y'(\zeta); \quad \xi < \zeta < \eta,$$
$$\leq 2^{\frac{-j}{2}-1}2^{-j}M, \quad \because y(\zeta) \leq M,$$
$$= 2^{\frac{-3j}{2}-1}M.$$

Therefore the equation (4.52) becomes,

$$\left\|y(\tau) - y_m(\tau)\right\|^2 = \sum_{n=2^j}^{\infty} C_i^2,$$

splitting the sum we have,

$$\left\|y(\tau) - y_m(\tau)\right\|^2 = \sum_{j=k+1}^{\infty} \left(\sum_{i=2^j}^{2^{j+1}-1} C_i^2 \right),$$

$$\leq \sum_{j=k+1}^{\infty} \left(\sum_{i=2^j}^{2^{j+1}-1} \left(2^{-\frac{3j}{2}-1}M \right)^2 \right) = \sum_{j=k+1}^{\infty} \left(\sum_{n=2^j}^{2^{j+1}-1} 2^{-3j-2}M^2 \right),$$

$$= \sum_{j=k+1}^{\infty} \left(2^{-3j-2}M^2 \sum_{i=2^j}^{2^{j+1}-1} \right),$$

$$= \sum_{j=k+1}^{\infty} 2^{-3j-2}M^2 \left(2^{j+1} - 1 - 2^j + 1 \right) = \sum_{j=k+1}^{\infty} 2^{-2j-2}M^2,$$

$$= M^2 \sum_{j=k+1}^{\infty} 2^{-2j-2}.$$

Using sum of the geometric series formula in above equation we have,

$$\left\|y(\tau) - y_m(\tau)\right\|^2 = \frac{2^{-2k-2}}{3}M^2,$$
$$= \frac{(m)^{-2}}{3}M^2 \quad \because m = 2^{k+1}.$$

Hence,

$$\left\|y(\tau) - y_m(\tau)\right\| = O\left(\frac{1}{m}\right).$$

So, one can manage to find the exact value of error bound $\frac{2^{-2k-2}}{3}M^2$, for the given partial sum in equation (4.22), if numerical value of M is given.

To estimate the value of M , suppose that we have a differentiable function $y(\tau)$ which is continuous on the interval $[0, 1]$. As first derivative of $y(\tau)$ is bounded and continuous on the interval $[0, 1]$, also $y' \in L^2[0, 1]$. So $y'(\tau)$ can be estimated as,

$$y'(\tau) \cong \sum_{i=0}^{m} C_i \Phi_i(\tau), \tag{4.27}$$

where $C_i = \langle y'(\tau), \Phi(\tau) \rangle$, also (4.27) can be written in the form of matrix as,

$$y'(\tau) \simeq C^T \Phi, \tag{4.28}$$

where $\boldsymbol{C} = [\boldsymbol{C}_0, \boldsymbol{C}_1, \boldsymbol{C}_2, \cdots, \boldsymbol{C}_{m-1}]^T$, and $\boldsymbol{\Phi} = [\boldsymbol{\Phi}_0, \boldsymbol{\Phi}_1, \boldsymbol{\Phi}_2, \cdots, \boldsymbol{\Phi}_{m-1}]$. Integration of equation (4.27), we have

$$y(\tau) - y(0) \simeq \sum_{i=0}^{m-1} \boldsymbol{C}_i \int_0^\tau \boldsymbol{\Phi}_i(\tau) d\tau. \tag{4.29}$$

As $\tau \in [0, 1]$, let us define the points

$$\tau_j = \frac{j - 0.01}{m}, \quad j = 1, 2, 3, \cdots, m.$$

By substituting τ_j in equation (4.29) we obtain,

$$y(\tau_j) - y(0) \simeq \sum_{i=0}^{m-1} \boldsymbol{C}_i \int_0^{\tau_j} \boldsymbol{\Phi}_i(\tau) d\tau, \tag{4.30}$$

we can write (4.30) in the form of matrix, as

$$\boldsymbol{Y} - \boldsymbol{Y}(0) = \boldsymbol{C}\boldsymbol{F}, \tag{4.31}$$

where $\boldsymbol{F} = \left[\int_0^{\tau_j} \boldsymbol{\Phi}_i(\tau) d\tau \right]_{0 \le i \le m-1, 1 \le j \le m}, \boldsymbol{C} = [\boldsymbol{C}_0, \boldsymbol{C}_1, \boldsymbol{C}_2, \cdots, \boldsymbol{C}_{m-1}]^T,$

$\boldsymbol{Y}(0) = [y(0), y(0), y(0), \cdots, y(0)]_{1 \times m}^T$, and $\boldsymbol{Y} = [y(\tau_1), y(\tau_2), y(\tau_3), \cdots, y(\tau_m)]^T$. We can determine the vector $\boldsymbol{C}$, putting this vector $\boldsymbol{C}$ into equation (4.27), $y'(\tau)$ can be calculated for each $\tau \in [0, 1]$. Assume $\tau_i \in [0, 1]$ and $y'(x_i)$ can be calculate for $i = 1, 2, 3, \cdots, l$, where l be the equidistant, then estimation of M may be considered as $\epsilon + \max |y'(x_i)|_{1 \le i \le l}$.

4.7 Numerical Results and Discussion

The numerical results and analysis of the suggested method for solving differential equations of fractional order are covered in this section. We study both initial value problem (IVP) and boundary value problem (BVP) problems using fractional order differentiable equations to demonstrate the effectiveness of this method.

Example 1. Consider the composite fractional oscillation equation.

$$^C_\tau D_0^\gamma y(\tau) + y(\tau) = f(\tau), \quad 0 < \gamma < 1. \tag{4.32}$$

Initial condition

$$y(0) = 0,$$

where

$$f(\tau) = \tau^2 + \frac{\Gamma(3)}{\Gamma(3-\gamma)} \tau^{2-\gamma}, \tag{4.33}$$

equation. (4.32) has the exact solution $y(\tau) = \tau^2$. Let

$$^C_\tau D_0^\gamma y(\tau) = C_m \Phi_m(\tau), \tag{4.34}$$

44

applying the initial condition $y(0) = 0$, we have

$$y(\tau) = C_{m_\tau} I_0^\gamma \Phi_m(\tau) + y(0), \tag{4.35}$$

substituting equations (4.34)-(4.35) in equation (4.32), we get

$$C_m \left[\Phi_m(\tau) + P_{m \times m}^\gamma \Phi_m(\tau) \right] = f_m \Phi_m(x), \tag{4.36}$$

where f_m is the evaluation of function $f(\tau)$ at collocation points, we plot the approximate and exact solutions at various γ values. The results are shown numerically in Table 4.1. It is evident from Figures 4.1, 4.2, 4.3, and 4.4 that, for each of the values of $\gamma = 0.15$ and $\gamma = 0.55$, the approximate solution agrees very well with the exact solution. By raising J, a good approximate solution for this problem can be found.
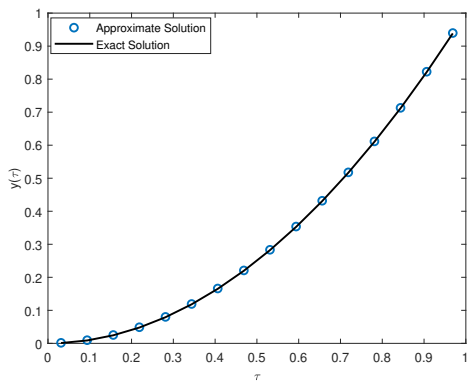

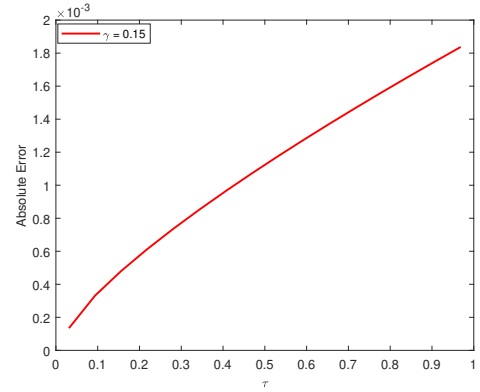Figure 4.1: Approximate and exact solution for $\gamma = 0.15$ when $J = 4$

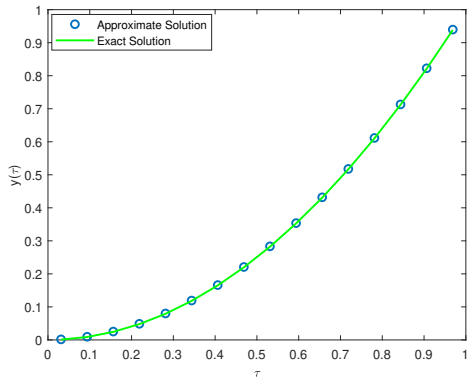Figure 4.2: Absolute errors at $\gamma = 0.15$ when $J = 4$

Figure 4.3: Approximate and exact solution for $\gamma = 0.55$ when $J = 4$
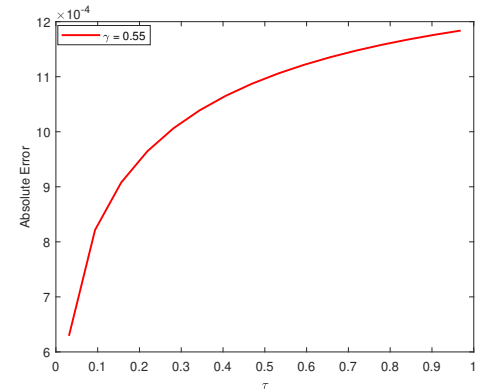

Figure 4.4: Absolute errors at $\gamma = 0.55$ when $J = 4$

Table 4.1. The Haar wavelet's absolute errors at $\gamma = 0.9$ with different choices of J.

$\gamma = 0.9$	$J = 6$	$J = 7$	$J = 8$	$J = 9$
τ	$\mathbb{E}_{\text{abs}}$	$\mathbb{E}_{\text{abs}}$	$\mathbb{E}_{\text{abs}}$	$\mathbb{E}_{\text{abs}}$
0	$5.9465e-05$	$1.4957e-05$	$3.7514e-06$	$9.3950e-07$
0.2	$5.1550e-05$	$1.3152e-05$	$3.3707e-06$	$8.6827e-07$
0.4	$4.3229e-05$	$1.1070e-05$	$2.8559e-06$	$7.3803e-07$
0.6	$3.6537e-05$	$9.4378e-06$	$2.4325e-06$	$6.2896e-07$
0.8	$3.1132e-05$	$8.0553e-06$	$2.0861e-06$	$5.4031e-07$
1	$2.7038e-05$	$6.9657e-06$	$1.8014e-06$	$4.6724e-07$

Example 2. Consider a fractional differential equation with boundary conditions:

$$^{\mathcal{C}}_{\tau}D_0^{\eta}y(\tau) + b(\tau)y(\tau) = f(\tau), \quad \tau \in [0,1], \quad 0 < \gamma \leq 1, \quad 1 < \eta \leq 2, \tag{4.37}$$

with boundary conditions.

$$y(0) = 0, \quad and \quad y(1) = \frac{1}{\Gamma(2)}.$$

For $b(\tau) = 1$, $f(\tau) = \frac{\Gamma(1+\kappa)}{\Gamma(2)\Gamma(1+\kappa-\eta)}x^{\kappa-\eta} + b(\tau)\frac{1}{\Gamma(2)}\tau^{\kappa}$, the exact solution of the differential equation is $y(\tau) = \frac{\tau^{\kappa}}{\Gamma(2)}$. To find a approximate solution of equation (4.37) by taking the approximation.

$$^{C}_{\tau}D_0^{\eta}y(\tau) = C_m\Phi_m(\tau), \tag{4.38}$$

integrating equation (4.38) on both sides, we have

$$y(\tau) = C_{m\tau}I_0^{\eta}\Phi_m(\tau) + c_1\tau + c_2, \tag{4.39}$$

by applying boundary conditions,

$$y(\tau) = C_{m\tau}I_0^{\eta}\Phi_m(\tau) + \left[\frac{1}{\Gamma(2)} - C_{m\tau}I_{0,1}^{\eta}\Phi_m(1)\right]\tau, \tag{4.40}$$

using (4.39) and (4.40) in (4.38) yields

$$C_m\left[\Phi_m(\tau) + AP_{m\times m}^{\eta}\Phi_m(\tau) - BP_{m\times m}^{\eta}\Phi_m(1)\right] = f_m\Phi_m(\tau), \tag{4.41}$$

where f_m is the evaluation of function $f(\tau)$ at collocation points and the matrices A, B are diagonal matrices of order $m \times m$, given by

$$A = \begin{bmatrix} a(\tau_1) & 0 & \cdots & 0 \\ 0 & a(\tau_2) & \cdots & 0 \\ \vdots & \vdots & \ddots & \vdots \\ 0 & 0 & \cdots & a(\tau_m) \end{bmatrix}, B = \begin{bmatrix} b(\tau_1) & 0 & \cdots & 0 \\ 0 & b(\tau_2) & \cdots & 0 \\ \vdots & \vdots & \ddots & \vdots \\ 0 & 0 & \cdots & b(\zeta_m) \end{bmatrix}.$$

By appling Haar wavelet method. In Figure 4.6, we examine absolute error at $\eta = 1.9$. We also discuss the exact and approximate solutions using the Haar wavelets approach at $\eta = 1.9$ in Figure 4.5. In Table 4.2, the numerical results are shown. A good approximation solution for this problem can be reached by raising J, as can be seen from Table 4.2, where the approximate answer is in strong agreement with the exact solution.
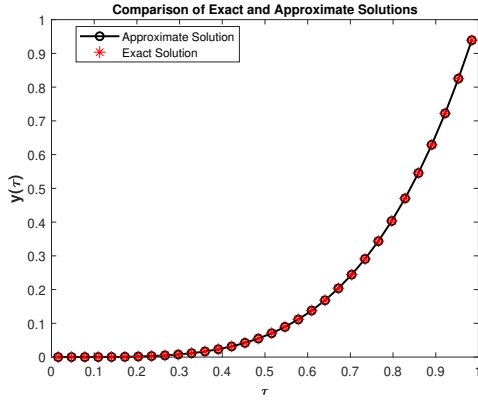
46

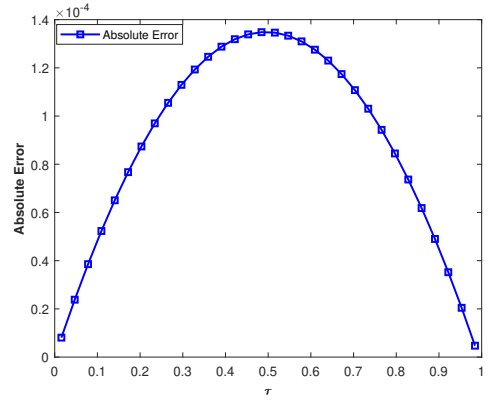Figure 4.5: Approximate and exact solutions for $\eta = 1.9$, $\kappa = 4$ when $J = 5$

Figure 4.6: The absolute error at $\eta = 1.9$, $\kappa = 4$ when $J = 5$

Table 4.2. The current scheme's absolute errors at a constant η vary with different choices of J.

$\eta = 1.3, \kappa = 4$	$J = 5$	$J = 6$	$J = 7$	$J = 8$
τ	$\mathbb{E}_{abs}$	$\mathbb{E}_{abs}$	$\mathbb{E}_{abs}$	$\mathbb{E}_{abs}$
0	3.4534e − 06	5.7024e − 07	8.4577e − 08	1.6138e − 09
0.2	1.8360e − 05	7.9851e − 06	2.6809e − 06	8.1013e − 07
0.4	9.5687e − 06	3.8729e − 06	2.2837e − 06	8.4842e − 07
0.6	8.7858e − 05	1.1096e − 05	6.9566e − 07	2.1654e − 07
0.8	1.8719e − 03	3.5078e − 05	6.0659e − 06	9.8426e − 07
1	3.1021e − 03	6.3665e − 05	1.3010e − 05	2.6518e − 06

4.8   Fast Algorithm with Haar Wavelet

In this section, we describe our approach to solving Caputo fractional partial differential equation with one dimension by combining a fast technique with Haar wavelets. Specifically, we discuss the intial and boundary conditions of the following Caputo fractional partial differential equation.

4.8.1   Fast Haar Wavelet method for solving Caputo Partial fractional differential equation with one dimension

Consider the following general form of Caputo partial fractional differential equation with one dimensions,

$$
\begin{aligned}
{}^{C}_{\zeta}D^{\gamma}_{0}y(\tau,\zeta) &= {}^{C}_{\tau}D^{\eta}_{0}y(\tau,\zeta) + y(\tau,\zeta) + f(\tau,\zeta), \\
y(\tau,o) &= y_0, \\
y(a_1,\zeta) = y_{a_1}, \quad &y(a_2,\zeta) = y_{a_2},
\end{aligned} \tag{4.42}
$$

47

where $-\infty < a_1 < \tau \leq a_2 < \infty, \quad 0 \leq \zeta < \infty$. Approximating the Caputo fractional derivative's highest order with a series of one-dimensional Haar wavelets,

$$_\zeta^C D_0^\eta y(\tau, \zeta_n) \approx \sum_{r=1}^{m} \sum_{k=0}^{m} C_{r,k}^n \Phi_{r,k}(\tau) = \mathbf{C_m} \mathbf{\Phi_m}(\tau), \qquad (4.43)$$

integral representation of equation (4.43) becomes

$$y(\tau, \zeta) = \boldsymbol{C}_{m\tau} \mathbb{I}_{a_1}^\eta \boldsymbol{\Phi}_m(\tau) + \tau c_1 + c_2, \qquad (4.44)$$

with the help of the boundary conditions, we get:

$$y(\tau, \zeta_n) = \boldsymbol{C}_{m\tau} \mathbb{I}_{a_1}^\eta \boldsymbol{\Phi}_m(\tau) + \frac{\tau}{a_2}((y_{a_2} - y_{a_1}) - \boldsymbol{C}_{m\tau} \mathbb{I}_{a_1,a_2}^\eta \boldsymbol{\Phi}_m(1)) + y_{a_1}, \qquad (4.45)$$

we used the formula shown in equation (2.48),

$$_\zeta^C D_0^\gamma y(\tau, \zeta_n) \approx \frac{1}{\Gamma(2-\gamma)} \left[\frac{y(\tau, \zeta_n) - y(\tau, \zeta_{n-1})}{(\Delta\zeta_n)^\gamma} \right] + \frac{1}{\Gamma(1-\gamma)} \left[\frac{y(\tau, \zeta_{n-1})}{(\Delta\zeta_n)^\gamma} - \frac{y(\tau, \zeta_0)}{(\zeta_n)^\gamma} \right]$$

$$- \gamma \sum_{i=1}^{Nexp} w_i \left(e^{-(si\Delta\zeta_n)} y_{hist,i}(\tau, \zeta_{n-1}) + \frac{e^{-(si\Delta\zeta_n)}}{si^2\Delta\zeta_{n-1}} \left[(e^{-si\Delta\zeta_{n-1}} - 1 + si\Delta\zeta_{n-1}) \right. \right.$$

$$\left. \left. y(\tau, \zeta_{n-1}) + \left(1 - e^{-si\Delta\zeta_{n-1}} - e^{-si\Delta\zeta_{n-1}} si\Delta\zeta_{n-1} \right) y(\tau, \zeta_{n-2}) \right] \right). \qquad (4.46)$$

Subtitute equations (4.43), (4.45) and (4.46) in equation (4.42), we get

$$C_m \left[\left(\frac{1}{\Delta\zeta^\gamma \Gamma(2-\gamma)} - 1 \right)_\tau \mathbb{I}_{a_1}^\eta \boldsymbol{\Phi}_m - (\frac{\tau}{a_2})(\frac{1}{\Delta\zeta^\gamma \Gamma(2-\gamma)} - 1)_\tau \mathbb{I}_{a_1,a_2}^\eta \boldsymbol{\Phi}_m(a_2)) - \boldsymbol{\Phi}_m(\tau) \right] =$$

$$f(x, \zeta_n) - \left(\frac{1}{\Delta\zeta^\gamma \Gamma(2-\gamma)} - 1 \right) [y(a_2) - y(a_1)] (\frac{\tau}{a_2}) + \frac{\gamma}{\Gamma(1-\gamma)} \sum_{i=1}^{Nexp} w_i y_{hist,i}(\tau, \zeta_n)$$

$$+ \frac{y(\tau, \zeta_0)}{(\zeta_n^\gamma)\Gamma(1-\gamma)} - \frac{y(\tau, \zeta_{n-1})}{(\Delta\zeta)^\gamma} \left(\frac{1}{\Gamma(1-\gamma)} - \frac{1}{\Gamma(2-\gamma)} \right), \qquad (4.47)$$

$$C_m \left[\boldsymbol{\Phi}_m(\tau) + A_\tau I_a^\eta \boldsymbol{\Phi}_m(\tau) + B_\tau I_{a_1,a_2}^\eta \boldsymbol{\Phi}_m(a_2) \right] = F_m \boldsymbol{\Phi}_m(\tau), \qquad (4.48)$$

where f_m is the evaluation of function $f(\tau)$ at collocation points and the matrices A, B are diagonal matrices of order $m \times m$, given by,

$$A = \begin{bmatrix} a(\tau_1) & 0 & \cdots & 0 \\ 0 & a(\tau_2) & \cdots & 0 \\ \vdots & \vdots & \ddots & \vdots \\ 0 & 0 & \cdots & a(\tau_m) \end{bmatrix}, B = \begin{bmatrix} b(\tau_1) & 0 & \cdots & 0 \\ 0 & b(\tau_2) & \cdots & 0 \\ \vdots & \vdots & \ddots & \vdots \\ 0 & 0 & \cdots & b(\tau_m) \end{bmatrix}.$$

The equation (4.48) is referred to as the Sylvester equation. To determine the value of $\mathbf{C}_m$ for each time step. Afterward, we can substitute the obtained value of $\mathbf{C}_m$ into either equation (4.45) in order to obtain an approximate solution.

4.9　Numerical Results and Discussion

In this section, we apply the proposed technique to solve some problems. Furthermore, we conduct a comparative analysis of the results, presented in a table, to evaluate the accuracy and efficiency of the suggested approach.

Example 3. Consider the Caputo fractional partial differential equation.

$$_\zeta^C D_0^\gamma y(\tau,\zeta) = b(\tau,\zeta)_\tau^C D_0^\eta y(\tau,\zeta) + c(\tau,\zeta)y(\tau,\zeta) + f(\tau,\zeta), \quad 0 < \gamma < 1, \quad 1 < \eta \le 2, \tag{4.49}$$

with initial and boundary conditions

$$y(\tau,0) = \cos(\pi)(\tau^3), \quad y(0,\zeta) = \cos(\pi)(\zeta^3) \quad and \quad y(1,\zeta) = \cos(\pi)(1+\zeta^3).$$

For fixed value of $\eta = 1.8, \gamma = 0.5$, $b(\tau,\zeta) = (1+\tau^2)\Gamma(1-\gamma)$ and $c(\tau,\zeta) = 1$,
$f(\tau,\zeta) = \cos(\pi)(\frac{\Gamma(4)}{\Gamma(4-\gamma)}\zeta^{3-\gamma} - \frac{\Gamma(4)}{\Gamma(4-\eta)}\tau^{3-\eta} - (\tau^3 + \zeta^3))$., then the exact solution to the problem is $y(\tau,\zeta) = (\tau^3 + \zeta^3)\cos(\pi)$. To find approximate solution of the equation (4.49) by the fast Haar wavelets method.

$$_\tau^C D_0^\eta y(\tau,\zeta) = C_m \boldsymbol{\Phi}_m(\tau). \tag{4.50}$$

The integral representation of equation (4.50) becomes

$$y(x,\zeta) = \boldsymbol{C}_{m\tau}\mathbb{I}_0^\eta \boldsymbol{\Phi}_m(\tau) + \tau c_1 + c_2, \tag{4.51}$$

utilizing the boundary conditions in equation (4.61) we get the values of
$c_1 = \cos(\pi) - \boldsymbol{C}_{m\tau}\mathbb{I}_{0,1}^\eta \boldsymbol{\Phi}_m(1)$ and $c_2 = \cos(\pi)\zeta^3$, we get:

$$y(\tau,\zeta_n) = \boldsymbol{C}_{m\tau}\mathbb{I}_0^\eta \boldsymbol{\Phi}_m(\tau) + \tau(\cos(\pi) - \boldsymbol{C}_{m\tau}\mathbb{I}_{0,1}^\eta \boldsymbol{\Phi}_m(1)) + (\cos(\pi))\zeta^3. \tag{4.52}$$

By using the formula which introduced in equation (2.49),

$$\begin{aligned}
_\zeta^C D_0^\gamma y(\tau,\zeta_n) \approx &\frac{1}{\Gamma(2-\gamma)}\left[\frac{y(\tau,\zeta_n) - y(\tau,\zeta_{n-1})}{(\Delta\zeta_n)^\gamma}\right] + \frac{1}{\Gamma(1-\gamma)}\left[\frac{y(\tau,\zeta_{n-1})}{(\Delta\zeta_n)^\gamma} - \frac{y(\tau,\zeta_0)}{(\zeta_n)^\gamma}\right. \\
&-\gamma\sum_{i=1}^{Nexp} w_i\left(e^{-(si\Delta\zeta_n)}y_{hist,i}(\tau,\zeta_{n-1}) + \frac{e^{-(si\Delta\zeta_n)}}{si^2\Delta\zeta_{n-1}}\left[(e^{-si\Delta\zeta_{n-1}} - 1 + si\Delta\zeta_{n-1})\right.\right. \\
&\left.\left.\left. y(\tau,\zeta_{n-1}) + \left(1 - e^{-si\Delta\zeta_{n-1}} - e^{-si\Delta\zeta_{n-1}}si\Delta\zeta_{n-1}\right)y(\tau,\zeta_{n-2})\right]\right)\right].
\end{aligned} \tag{4.53}$$

Subtitute equations (4.51), (4.52) and (4.53) in equation (4.49), we get

$$C_m\left[\left(\frac{1}{\Delta\zeta^\gamma\Gamma(2-\gamma)} - c(\tau,\zeta)\right)_\tau\mathbb{I}_0^\eta \boldsymbol{\Phi}_m(\tau) + \frac{\tau}{\Delta\zeta^\gamma\Gamma(2-\gamma)}(_\tau\mathbb{I}_{0,1}^\eta \boldsymbol{\Phi}_m(1)) - \boldsymbol{b}(\boldsymbol{\tau},\boldsymbol{\zeta})\boldsymbol{\Phi}_m(\tau)\right] =$$

$$f(x,\zeta_n) - \left(\frac{1}{\Delta\zeta^\gamma\Gamma(2-\gamma)} - c(\tau,\zeta)\right)\left[\cos(\pi)(1+(\zeta_n)^3)\right] + \frac{\gamma}{\Gamma(1-\gamma)}\sum_{i=1}^{Nexp} w_i y_{hist,i}(\tau,\zeta_n)$$

$$+ \frac{y(\tau,\zeta_0)}{(\zeta_n{}^\gamma)\Gamma(1-\gamma)} - \frac{y(\tau,\zeta_{n-1})}{(\Delta\zeta)^\gamma}\left(\frac{1}{\Gamma(1-\gamma)} - \frac{1}{\Gamma(2-\gamma)}\right), \tag{4.54}$$

$$C_m \left[\boldsymbol{A}_\tau \mathbb{I}_0^\eta \boldsymbol{\Phi}_m(\tau) + (\boldsymbol{B}_\tau \mathbb{I}_{0,1}^\eta \boldsymbol{\Phi}_m(1)) - \boldsymbol{C}\Phi_m(\tau) \right] = \boldsymbol{f_m} \tag{4.55}$$

where f_m is the evaluation of function $f(\tau)$ at collocation points and the matrices A, B and C are diagonal matrices of order $m \times m$, given by,

$$A = \begin{bmatrix} a(\tau_1) & 0 & \cdots & 0 \\ 0 & a(\tau_2) & \cdots & 0 \\ \vdots & \vdots & \ddots & \vdots \\ 0 & 0 & \cdots & a(\tau_m) \end{bmatrix}, B = \begin{bmatrix} b(\tau_1) & 0 & \cdots & 0 \\ 0 & b(\tau_2) & \cdots & 0 \\ \vdots & \vdots & \ddots & \vdots \\ 0 & 0 & \cdots & b(\zeta_m) \end{bmatrix}$$

and

$$C = \begin{bmatrix} c(\tau_1) & 0 & \cdots & 0 \\ 0 & c(\tau_2) & \cdots & 0 \\ \vdots & \vdots & \ddots & \vdots \\ 0 & 0 & \cdots & c(\tau_m) \end{bmatrix}.$$

The equation (4.55) is known as the sylvester equation and the exact their approximate solution for $\eta = 1.5$,$\gamma = 0.4$ and $j = 9$ are shown respectively in Figure 4.7 and Figure 4.8 and absolute error is also ploted for the values $\eta = 1.5$,$\gamma = 0.4$ and $j = 6$ in Figure 4.9 with time step 64.
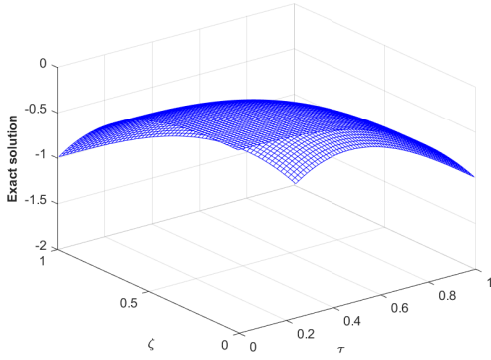

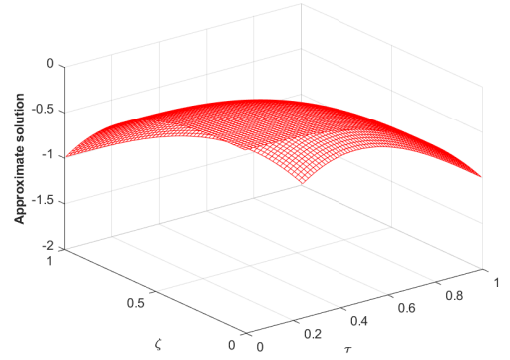Figure 4.7: Exact solution at $\eta = 1.5$, $\gamma = 0.4$ and $J = 6$

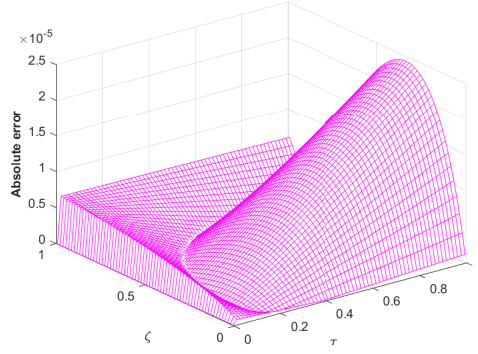Figure 4.8: Approximate solution at $\eta = 1.5$, $\gamma = 0.4$ and $J = 6$

Figure 4.9: The absolute error at $\eta = 1.5$, $\gamma = 0.4$ and $J = 6$

Table 4.3. The fast Haar wavelet's absolute errors at $\eta = 1.5$, $\gamma = 0.4$ with different values of J.

$\eta = 1.5, \gamma = 0.4$	$J = 3$	$J = 4$	$J = 5$
(ζ, τ)	$\mathbb{E}_{abs}$	$\mathbb{E}_{abs}$	$\mathbb{E}_{abs}$
(0.2,0.1)	$1.1330e - 03$	$1.3103e - 04$	$1.3536e - 05$
(0.4,0.1)	$1.0887e - 03$	$1.2710e - 04$	$1.1067e - 05$
(0.6,0.1)	$1.0847e - 03$	$1.2467e - 04$	$8.2889e - 06$
(0.8,0.1)	$1.0801e - 03$	$1.2269e - 04$	$5.9243e - 06$
(1.0,0.1)	$1.0785e - 03$	$1.2092e - 04$	$3.5627e - 06$

Example 4. Consider the Caputo fractional partial differential equation.

$$ {}^C_\zeta D_0^\gamma y(\tau, \zeta) = m(\tau, \zeta) {}^C_\tau D_0^\eta y(\tau, \zeta) + n(\tau, \zeta) y(\tau, \zeta) + s(\tau, \zeta), \quad 0 < \gamma < 1, \quad 1 < \eta \le 2, \tag{4.56} $$

with initial and boundary conditions

$$ y(\tau, 0) = 2(\gamma + 1) \quad y(0, \zeta) = (\gamma + 1)(\zeta^\eta + 2) \quad and \quad y(1, \zeta) = (\gamma + 1)(\zeta^\eta + 2) $$

For fixed value of $\eta = 1.5, \gamma = 0.2$, $m(\tau, \zeta) = (\tau^\eta + \eta + cos(2))$, $n(\tau, \zeta) = 1 + \eta$ and
$s(\tau, \zeta) = (\gamma + 1) \left(\frac{\Gamma(\eta+1)}{\Gamma(\eta+1-\gamma)} (\zeta^{\eta-\gamma}) - n(\tau, \zeta)(\zeta^\eta + 2) \right)$, then exact solution to the problem is
$y(\tau, \zeta) = (\gamma + 1)(\zeta^\eta + 2)$, find the approximate solution of the equation (4.56) by the fast Haar
wavelets method.

$$ {}^C_\tau D_0^\eta y(\tau, \zeta) = C_m \mathbf{\Phi}_m(\tau). \tag{4.57} $$

The integral representation of equation (4.57) becomes,

$$ y(x, \zeta) = \boldsymbol{C}_{m\tau} \mathbb{I}_0^\eta \mathbf{\Phi}_m(\tau) + \tau c_1 + c_2, \tag{4.58} $$

utilizing the boundary conditions in equation (4.58) we get the values of
$c_1 = (\gamma + 1)\zeta^\eta - \boldsymbol{C}_{m\tau} \mathbb{I}_{0,1}^\eta \mathbf{\Phi}_m(1)$ and $c_2 = (\gamma + 1)(\zeta^\eta + 2)$, substituting these values into equation
(4.58), we get:

$$y(\tau,\zeta_n) = \boldsymbol{C}_{m\,\tau}\mathbb{I}_0^\eta\boldsymbol{\Phi}_m(\tau) + \tau((\gamma+1)\zeta^\eta - \boldsymbol{C}_{m\,\tau}\mathbb{I}_{0,1}^\eta\boldsymbol{\Phi}_m(1)) + (\gamma+1)(\zeta^\eta+2),\qquad(4.59)$$

by using the formula which introduced in equation (2.58),

$$\begin{aligned}
{}_\zeta^C D_0^\gamma y(\tau,\zeta_n) \approx & \frac{1}{\Gamma(2-\gamma)}\left[\frac{y(\tau,\zeta_n)-y(\tau,\zeta_{n-1})}{(\Delta\zeta_n)^\gamma}\right] + \frac{1}{\Gamma(1-\gamma)}\left[\frac{y(\tau,\zeta_{n-1})}{(\Delta\zeta_n)^\gamma} - \frac{y(\tau,\zeta_0)}{(\zeta_n)^\gamma}\right]\\
& -\gamma\sum_{i=1}^{Nexp} w_i\left(e^{-(si\Delta\zeta_n)}y_{hist,i}(\tau,\zeta_{n-1}) + \frac{e^{-(si\Delta\zeta_n)}}{si^2\Delta\zeta_{n-1}}\left[(e^{-si\Delta\zeta_{n-1}}-1+si\Delta\zeta_{n-1})\right.\right.\\
& \left.\left. y(\tau,\zeta_{n-1}) + \left(1-e^{-si\Delta\zeta_{n-1}}-e^{-si\Delta\zeta_{n-1}}si\Delta\zeta_{n-1}\right)y(\tau,\zeta_{n-2})\right]\right).
\end{aligned}\qquad(4.60)$$

Subtitute equations (4.57), (4.59) and (4.60) in equation (4.56), we get

$$C_m\left[\left(\frac{1}{\Delta\zeta^\gamma\Gamma(2-\gamma)} - n(\tau,\zeta)\right){}_\tau\mathbb{I}_0^\eta\boldsymbol{\Phi}_m(\tau) + \frac{\tau}{\Delta\zeta^\gamma\Gamma(2-\gamma)}({}_\tau\mathbb{I}_{0,1}^\eta\boldsymbol{\Phi}_m(1)) - \boldsymbol{m}(\boldsymbol{\tau},\boldsymbol{\zeta})\boldsymbol{\Phi}_m(\tau)\right] =$$

$$f(x,\zeta_n) + \left(\frac{1}{\Delta\zeta^\gamma\Gamma(2-\gamma)} - n(\tau,\zeta)\right)\left[(\gamma+1)(\zeta^n+2)\right] + \frac{\gamma}{\Gamma(1-\gamma)}\sum_{i=1}^{Nexp} w_i y_{hist,i}(\tau,\zeta_n)$$

$$+ \frac{y(\tau,\zeta_0)}{(\zeta_n{}^\gamma)\Gamma(1-\gamma)} - \frac{y(\tau,\zeta_{n-1})}{(\Delta\zeta)^\gamma}\left(\frac{1}{\Gamma(1-\gamma)} - \frac{1}{\Gamma(2-\gamma)}\right),\qquad(4.61)$$

$$C_m\left[\boldsymbol{A}_\tau\mathbb{I}_0^\eta\boldsymbol{\Phi}_m(\tau) + \boldsymbol{B}_\tau\mathbb{I}_{0,1}^\eta\boldsymbol{\Phi}_m(1) - \boldsymbol{C}\boldsymbol{\Phi}_m(\tau)\right] = \boldsymbol{S_m},\qquad(4.62)$$

where S_m is the evaluation of function $S(\tau)$ at collocation points and the matrices A, B and C are diagonal matrices of order $m\times m$, given by

$$A = \begin{bmatrix} a(\tau_1) & 0 & \cdots & 0\\ 0 & a(\tau_2) & \cdots & 0\\ \vdots & \vdots & \ddots & \vdots\\ 0 & 0 & \cdots & a(\tau_m)\end{bmatrix}, B = \begin{bmatrix} b(\tau_1) & 0 & \cdots & 0\\ 0 & b(\tau_2) & \cdots & 0\\ \vdots & \vdots & \ddots & \vdots\\ 0 & 0 & \cdots & b(\zeta_m)\end{bmatrix}$$

and

$$C = \begin{bmatrix} c(\tau_1) & 0 & \cdots & 0\\ 0 & c(\tau_2) & \cdots & 0\\ \vdots & \vdots & \ddots & \vdots\\ 0 & 0 & \cdots & c(\tau_m)\end{bmatrix}.$$

The equation (4.62) is known as the sylvester equation and the exact their approximate solution for $\eta = 1.4$, $\gamma = 0.4$ and $j = 6$ are shown respectively in Figure 4.10 and Figure 4.11 and absolute error is also ploted for the values $\eta = 1.4$, $\gamma = 0.4$ and $j = 6$ in Figure 4.12 with time step 64.
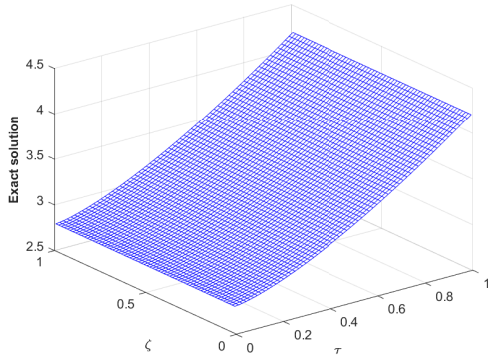
Figure 4.10: Exact solution by choosing $\eta = 1.4$, $\gamma = 0.4$ and $J = 6$
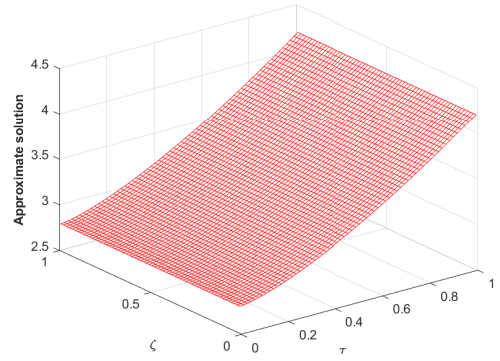

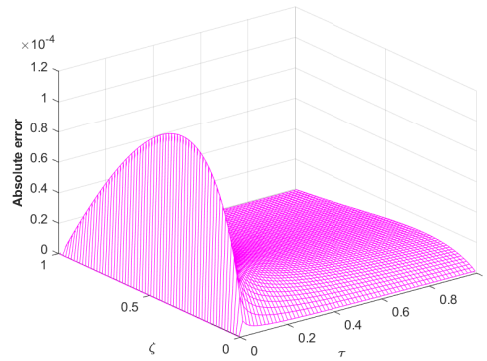Figure 4.11: Approximate solution at $\eta = 1.4$, $\gamma = 0.4$ and $J = 6$

Figure 4.12: Absolute error at $\eta = 1.4$, $\gamma = 0.4$ and $j = 6$

Table 4.4. The fast Haar wavelet's absolute errors at $\eta = 1.3$, $\gamma = 0.3$ with different values of J.

$\eta = 1.3, \gamma = 0.3$	$J = 3$	$J = 4$	$J = 5$
(ζ, τ)	$\mathbb{E}_{abs}$	$\mathbb{E}_{abs}$	$\mathbb{E}_{abs}$
(0.2,0.70)	$2.7355e - 06$	$2.7040e - 06$	$2.7121e - 06$
(0.4,0.70)	$1.7408e - 06$	$1.8974e - 06$	$1.9827e - 06$
(0.6,0.70)	$1.0263e - 06$	$8.4308e - 07$	$7.6310e - 07$
(0.8,0.70)	$1.0177e - 07$	$1.5103e - 07$	$1.1287e - 07$
(1.0,0.70)	$1.5100e - 08$	$1.9957e - 08$	$1.2774e - 08$

4.10   Conclusion

It has been found that the Haar wavelets method performed well when used to solve various Caputo fractional differential equations, including initial value problems (IVPs) and boundary value problems (BVPs). Numerical solutions of these equations converged to the exact solutions in our examples. The fast Haar wavelets method also proved effective in solving partial differential initial boundary value equations. From the examples and comparisons shown, it is demonstrated that both the Haar wavelets and fast Haar wavelets techniques are capable of handling a variety of fractional order differential equations effectively, providing reliable and accurate results.

Chapter 5

Summary

In first chapter, we cover the history and basics of fractional calculus. We also explain the Gamma function in detail, highlighting its key properties. The chapter introduces several important fractional operators. Additionally, we provide an overview of wavelet analysis, discussing its properties and different types of wavelets. In second chapter, we explore a fast evaluation technique for solving Caputo fractional differential equations and demonstrate its reliability. We also discuss another approximation method for the Caputo-Hadamard differential equations using the fast evaluation technique, focusing on a specific problem to illustrate its applicability. In third chapter, we introduced a numerical technique for solving linear ordinary fractional differential equations with initial value problems (IVPs) and boundary value problems (BVPs). This method, known as the Hadmarad Gagenbauer wavelets method, was developed to evaluate its effectiveness and accuracy. We present graphical and tabular results from various numerical experiments and compare our method with exact solutions. Based on this evidence, we conclude that the Hadmarad wavelets method is not only computationally efficient but also sound and accurate.

In fourth chapter, we explored numerical methods for solving Caputo Ordinary and Partial fractional differential equations. For Caputo Ordinary fractional differential equations, we utilized the Haar wavelet method, presenting figures and tables that demonstrate the effectiveness of this approach. Additionally, we introduced a novel approach called the Fast Haar Wavelet Method, which we applied to solve partial fractional differential equations examples. By comparing the exact and approximate solutions through figures and tables, we observed good reliability in the Haar wavelet method for Ordinary fractional differential equations examples. Furthermore, we concluded that the Fast Haar Wavelet Method is both reliable and closely aligned with exact solution.

The accuracy of the proposed scheme is then verified by making comparisons. It has been observed that the accuracy of the approximate solution provided by the proposed Haar wavelets method enhances by increasing the values of J. In the case of partial fractional differential equations, the solution by the proposed scheme converges to the exact solution as the values of J increase.

Bibliography

[1] Sikora, B. (2023). Remarks on the Caputo fractional derivative. Minut, 5, 76-84.

[2] Lacroix, S. F. (1797). Traité du calcul différentiel et du calcul intégral (Vol. 1). JBM Duprat.

[3] Debnath, L., Grum, W. J. (1988). The fractional calculus and its role in the synthesis of special functions: Part I. International Journal of Mathematical Education in Science and Technology, 19(2), 215-230.

[4] Hardy, G. H., Littlewood, J. E. (1928). Some properties of fractional integrals. I. Mathematische Zeitschrift, 27(1), 565-606.

[5] Kilbas, A. A., Srivastava, H. M., Trujillo, J. J. (2006). Theory and applications of fractional differential equations (Vol. 204). Elsevier.

[6] Magin, R. (2004). Fractional calculus in bioengineering, part 1. Critical Reviews™ in Biomedical Engineering, 32(1).

[7] Podlubny, I. (1998). Fractional differential equations: an introduction to fractional derivatives, fractional differential equations, to methods of their solution and some of their applications. Elsevier.

[8] Samko, S. G. (1993). Fractional integrals and derivatives. Theory and applications.

[9] Katugampola, U. N. (2011). New approach to a generalized fractional integral. Applied mathematics and computation, 218(3), 860-865.

[10] Katugampola, U. N. (2011). A new approach to generalized fractional derivatives. *arXiv preprint arXiv:1106.0965.*

[11] He, J. (1997). A new approach to nonlinear partial differential equations. *Communications in Nonlinear Science and Numerical Simulation, 2*(4), 230-235. Elsevier.

[12] He, J.-H. (1998). Approximate analytical solution for seepage flow with fractional derivatives in porous media. *Computer Methods in Applied Mechanics and Engineering, 167*(1-2), 57-68. Elsevier.

[13] He, J.-H. (2006). Some asymptotic methods for strongly nonlinear equations. *International Journal of Modern Physics B, 20*(10), 1141-1199. World Scientific.

[14] Anh, V. V., & Leonenko, N. N. (2001). Spectral analysis of fractional kinetic equations with random data. *Journal of Statistical Physics, 104*, 1349-1387. Springer.

[15] Blaszczyk, T., Ciesielski, M., Klimek, M., & Leszczynski, J. (2011). Numerical solution of fractional oscillator equation. *Applied Mathematics and Computation, 218*(6), 2480-2488. Elsevier.

[16] Khan, N. A., Ara, A., Ali, S. A., & Mahmood, A. (2009). Analytical study of Navier-Stokes equation with fractional orders using He's homotopy perturbation and variational iteration methods. *International Journal of Nonlinear Sciences and Numerical Simulation, 10*(9), 1127-1134. De Gruyter.

[17] Schulz, B. M., & Schulz, M. (2006). Numerical investigations of anomalous diffusion effects in glasses. *Journal of Non-Crystalline Solids, 352*(42-49), 4884-4887. Elsevier.

[18] Sierociuk, D., Dzieliński, A., Sarwas, G., Petras, I., Podlubny, I., & Skovranek, T. (2013). Modelling heat transfer in heterogeneous media using fractional calculus. *Philosophical Transactions of the Royal Society A: Mathematical, Physical and Engineering Sciences, 371*(1990), 20120146. The Royal Society Publishing.

[19] He, J.-H. (1999). Some applications of nonlinear fractional differential equations and their approximations. *Bull. Sci. Technol, 15*(2), 86-90.

[20] Magin, R. (2004). Fractional calculus in bioengineering, part 2. *Critical Reviews™ in Biomedical Engineering, 32*(2). Begel House Inc.

[21] Engheta, N. (1996). On fractional calculus and fractional multipoles in electromagnetism. *IEEE Transactions on Antennas and Propagation, 44*(4), 554-566. IEEE.

[22] Sebah, P., & Gourdon, X. (2002). Introduction to the gamma function. *American Journal of Scientific Research*, 2-18.

[23] Diethelm, K., & Ford, N. J. (2010). The analysis of fractional differential equations. *Lecture Notes in Mathematics, 2004*.

[24] Li, C., Qian, D., & Chen, Y. (2011). On Riemann-Liouville and Caputo derivatives. *Discrete Dynamics in Nature and Society, 2011*(1), 562494. Wiley Online Library.

[25] Jarad, F., Abdeljawad, T., & Baleanu, D. (2012). Caputo-type modification of the Hadamard fractional derivatives. *Advances in Difference Equations, 2012*, 1-8. Springer.

[26] Kilbas, A. A. (2001). Hadamard-type fractional calculus. *J. Korean Math. Soc, 38*(6), 1191-1204. Citeseer.

[27] Feichtinger, H. G., & Gröchenig, K. (1992). Gabor wavelets and the Heisenberg group: Gabor expansions and short time Fourier transform from the group theoretical point of view. *Wavelets: A Tutorial in Theory and Applications, 2*, 359-398. Academic Press, Boston.

[28] Guido, R. C. (2022). Wavelets behind the scenes: Practical aspects, insights, and perspectives. *Physics Reports, 985*, 1-23. Elsevier.

[29] Cohen, A. (2000). Wavelet methods in numerical analysis. *Handbook of Numerical Analysis, 7*, 417-711. Elsevier.

[30] Hu, Y., Li, F., Li, H., & Liu, C. (2017). An enhanced empirical wavelet transform for noisy and non-stationary signal processing. *Digital Signal Processing, 60*, 220-229. Elsevier.

[31] Hess-Nielsen, N., & Wickerhauser, M. V. (1996). Wavelets and time-frequency analysis. *Proceedings of the IEEE, 84*(4), 523-540. IEEE.

[32] Lepik, Ü. (2005). Numerical solution of differential equations using Haar wavelets. *Mathematics and Computers in Simulation, 68*(2), 127-143. Elsevier.

[33] Yousefi, S. A. (2006). Legendre wavelets method for solving differential equations of Lane–Emden type. *Applied Mathematics and Computation, 181*(2), 1417-1422. Elsevier.

[34] Heydari, M. H., Hooshmandasl, M. R., Maalek Ghaini, F. M., & Mohammadi, F. (2012). Wavelet collocation method for solving multiorder fractional differential equations. *Journal of Applied Mathematics, 2012*(1), 542401. Wiley Online Library.

[35] Aguiar-Conraria, L., & Soares, M. J. (2014). The continuous wavelet transform: Moving beyond uni-and bivariate analysis. *Journal of Economic Surveys, 28*(2), 344-375. Wiley Online Library.

[36] Valens, C. (1999). A really friendly guide to wavelets.

[37] Poularikas, A. D. (2000). The Transforms and Applications Handbook: Ed. Alexander D. Poularikas Boca Raton: CRC Press LLC, 2000.

[38] Pervaiz, N., Aziz, I. (2020). Haar wavelet approximation for the solution of cubic nonlinear Schrodinger equations. Physica A: Statistical Mechanics and its Applications, 545, 123738.

[39] Saeed, U., ur Rehman, M. (2013). Haar wavelet–quasilinearization technique for fractional non-linear differential equations. Applied Mathematics and Computation, 220, 630-648.

[40] Yuttanan, B., Razzaghi, M., Vo, T. N. (2021). Legendre wavelet method for fractional delay differential equations. Applied Numerical Mathematics, 168, 127-142.

[41] Wang, Z., Wang, C., Ding, L., Wang, Z., Liang, S. (2022). Parameter identification of fractional-order time delay system based on Legendre wavelet. Mechanical Systems and Signal Processing, 163, 108141.

[42] Ghanbari, G., Razzaghi, M. (2022). Numerical solutions for fractional optimal control problems by using generalised fractional-order Chebyshev wavelets. International Journal of Systems Science, 53(4), 778-792.

[43] Gohar, M., Li, C., Li, Z. (2020). Finite difference methods for Caputo–Hadamard fractional differential equations. Mediterranean Journal of Mathematics, 17(6), 194.

[44] Jiang, S., Zhang, J., Zhang, Q., Zhang, Z. (2017). Fast evaluation of the Caputo fractional derivative and its applications to fractional diffusion equations. Communications in Computational Physics, 21(3), 650-678.

[45] Beylkin, G., Monzón, L. (2010). Approximation by exponential sums revisited. Applied and Computational Harmonic Analysis, 28(2), 131-149.

[46] ur Rehman, M., Saeed, U. (2015). Gegenbauer wavelets operational matrix method for fractional differential equations. Journal of the Korean Mathematical Society, 52(5), 1069-1096.

[47] Hariharan, G., Kannan, K. (2013). An overview of Haar wavelet method for solving differential and integral equations. World Applied Sciences Journal, 23(12), 1-14.

[48] Babolian, E., Shahsavaran, A. (2009). Numerical solution of nonlinear Fredholm integral equations of the second kind using Haar wavelets. Journal of Computational and Applied Mathematics, 225(1), 87-95.

[49] Saeed, U. (2022). A wavelet method for solving Caputo–Hadamard fractional differential equation. Engineering Computations, 39(2), 650-671.

[50] Guo, B., Xu, Q., Zhu, A. (2016). A second-order finite difference method for two-dimensional fractional percolation equations. Communications in Computational Physics, 19(3), 733-757.

[51] Ali, A., Minamoto, T., Saeed, U., Rehman, M. U. (2021). -Haar wavelets method for numerically solving fractional differential equations. Engineering Computations, 38(2), 1037-1056.

[52] Mechee, M. S., Al-Shaher, O. I., Al-Juaifri, G. A. (2019, April). Haar wavelet technique for solving fractional differential equations with an application. In AIP Conference Proceedings (Vol. 2086, No. 1). AIP Publishing.

[53] Ismail, M., Rehman, M. U., Saeed, U. (2020). Green-Haar method for fractional partial differential equations. Engineering Computations, 37(4), 1473-1490.

[54] Zhang, J., Tang, Y., Huang, J. (2023). A fast Euler-Maruyama method for fractional stochastic differential equations. Journal of Applied Mathematics and Computing, 69(1), 273-291.

[55] Bhrawy, A. H., Doha, E. H., Baleanu, D., Ezz-Eldien, S. S. (2015). A spectral tau algorithm based on Jacobi operational matrix for numerical solution of time fractional diffusion-wave equations. Journal of Computational Physics, 293, 142-156.

[56] Çelik, İ., Öztürk, H. K. (2021). Heat transfer and velocity in the squeezing flow between two parallel disks by Gegenbauer Wavelet Collocation Method. Archive of Applied Mechanics, 91(1), 443-461.

[57] Ozdemir, N., Secer, A., Bayram, M. (2019). The Gegenbauer wavelets-based computational methods for the coupled system of Burgers' equations with time-fractional derivative. Mathematics, 7(6), 486.

[58] Srivastava, H. M., Shah, F. A., Abass, R. (2019). An application of the Gegenbauer wavelet method for the numerical solution of the fractional Bagley-Torvik equation. Russian Journal of Mathematical Physics, 26(1), 77-93.